IOP Publishing Journal of Physics A: Mathematical and Theoretical
J. Phys. A: Math. Theor. **48** (2015) 325201 (28pp) doi:10.1088/1751-8113/48/32/325201

# Dimer with gain and loss: Integrability and $\mathcal{PT}$-symmetry restoration

**I V Barashenkov[1,4], D E Pelinovsky[2] and P Dubard[3]**

[1] Centre for Theoretical and Mathematical Physics, University of Cape Town, Rondebosch 7701, South Africa and Joint Institute for Nuclear Research, Dubna, Russia
[2] Department of Mathematics, McMaster University, Hamilton ON, Canada, L8S 4K1 and Department of Applied Mathematics, Nizhny Novgorod State Technical University, Nizhny Novgorod, Russia
[3] Department of Mathematics, University of Cape Town, Rondebosch 7701, South Africa

E-mail: igor.barashenkov@uct.ac.za

Received 12 March 2015, revised 17 June 2015
Accepted for publication 22 June 2015
Published 23 July 2015


**Abstract**

A $\mathcal{PT}$-symmetric nonlinear Schrödinger dimer is a two-site discrete nonlinear Schrödinger equation with one site losing and the other one gaining energy at the same rate. In this paper, two four-parameter families of cubic $\mathcal{PT}$-symmetric dimers are constructed as gain–loss extensions of their conservative, Hamiltonian, counterparts. We prove that all these damped-driven equations define completely integrable Hamiltonian systems. The second aim of our study is to identify nonlinearities that give rise to the spontaneous $\mathcal{PT}$-symmetry restoration. When the symmetry of the underlying linear dimer is broken and an unstable small perturbation starts to grow, the nonlinear coupling of the required type will divert an increasingly large percentage of energy from the gaining to the losing site. As a result, the exponential growth will be saturated and all trajectories remain trapped in a finite part of the phase space regardless of the value of the gain–loss coefficient.

Keywords: $\mathcal{PT}$-symmetry, nonlinear Schrödinger dimer, Hamiltonian structure, complete integrability, gain and loss, trajectory confinement, spontaneous symmetry restoration

(Some figures may appear in colour only in the online journal)

[4] Author to whom any correspondence should be addressed.

## 1. Introduction

The nonlinear Schrödinger *dimer* is a code name for the discrete nonlinear Schrödinger equation defined on a lattice consisting just of two sites:

$$\begin{aligned} \mathrm{i}\dot{u} + v &= F\left(u,\, u^*,\, v,\, v^*\right), \\ \mathrm{i}\dot{v} + u &= G\left(u,\, u^*,\, v,\, v^*\right). \end{aligned} \tag{1}$$

Here and in what follows, the overdot denotes the derivative with respect to $t$ and the asterisk indicates complete conjugation.

The dimer (1) is one of the simplest (and hence most heavily used) models of a coupled bimodal structure. In optics, the system (1) describes the directional coupler—a pair of parallel waveguides coupled through their evanescent fields. In this context, $u$ and $v$ are the complex amplitudes of stationary light beams in the waveguides and $t$ measures the distance along their parallel cores [1–3].

When the same system is employed in the studies of the Bose–Einstein condensates, $u$ and $v$ stand for the amplitudes of the mean-field condensate wave functions localized in the left and right well of a double-well potential [4] (or of their symmetric and antisymmetric combinations [5]). In this application, $t$ has the meaning of time.

The nonlinear Schrödinger dimers were also utilized in the solid state physics [6–8] and in the context of electric lattices [8].

Typically, the dimer arises as an amplitude equation; that is, $u$ and $v$ represent slowly changing amplitudes of some oscillatory variables $x$ and $y$:

$$x(\tau) = u(t)\mathrm{e}^{\mathrm{i}\omega\tau} + u^*(t)\mathrm{e}^{-\mathrm{i}\omega\tau} + \ldots, \quad y(\tau) = v(t)\mathrm{e}^{\mathrm{i}\omega\tau} + v^*(t)\mathrm{e}^{-\mathrm{i}\omega\tau} + \ldots . .$$

Here $t = \epsilon^2\tau$, $\epsilon^2$ is a small parameter, and the dots stand for small anharmonic corrections. The invariance of the optical or atomic structure with respect to translations in $\tau$ is inherited by the amplitude equations as the invariance under simultaneous phase shifts in $u$ and $v$. In other words, physically meaningful nonlinearities have to satisfy

$$\begin{aligned} F\left(\mathrm{e}^{\mathrm{i}\phi}u,\, \mathrm{e}^{-\mathrm{i}\phi}u^*,\, \mathrm{e}^{\mathrm{i}\phi}v,\, \mathrm{e}^{-\mathrm{i}\phi}v^*\right) &= \mathrm{e}^{\mathrm{i}\phi}F\left(u,\, u^*,\, v,\, v^*\right), \\ G\left(\mathrm{e}^{i\phi}u,\, \mathrm{e}^{-\mathrm{i}\phi}u^*,\, \mathrm{e}^{\mathrm{i}\phi}v,\, \mathrm{e}^{-\mathrm{i}\phi}v^*\right) &= \mathrm{e}^{\mathrm{i}\phi}G\left(u,\, u^*,\, v,\, v^*\right) \end{aligned} \tag{2}$$

for any real $\phi$.

Another property of the dimer dictated by physics, is conservation of energy which gives rise to an underlying Hamiltonian structure. There are two main types of Hamiltonian formulations admitted by the dimers. One class of Hamiltonian dimers has the *straight-gradient* form

$$\mathrm{i}\frac{\mathrm{d}u}{\mathrm{d}t} = \frac{\partial\mathcal{H}}{\partial u^*}, \qquad \mathrm{i}\frac{\mathrm{d}v}{\mathrm{d}t} = \frac{\partial\mathcal{H}}{\partial v^*}. \tag{3}$$

Here $\mathcal{H}$ is the Hamilton function while the canonical coordinate-momentum pairs are $(u,\, u^*)$ and $(v,\, v^*)$. Alternatively, $u$ can be paired with $v^*$, while $u^*$ play the role of momentum conjugate to $v$:

$$\mathrm{i}\frac{\mathrm{d}u}{\mathrm{d}t} = \frac{\partial\mathfrak{H}}{\partial v^*}, \qquad \mathrm{i}\frac{\mathrm{d}v}{\mathrm{d}t} = \frac{\partial\mathfrak{H}}{\partial u^*}. \tag{4}$$

(This time we use a different notation for the Hamilton function to keep the treatment of the two cases separate.) In what follows, we are referring to equations of the form (4) as the *cross-gradient* systems.

The last requirement is that of the left–right symmetry (the parity symmetry) of the system. This requirement arises if the two elements making up the dimer (two waveguides or

two potential wells) are identical. Mathematically, it reduces to the invariance under the permutation of $u$ and $v$ in (1):

$$F\left(u,\, u^*,\, v,\, v^*\right) = G\left(v,\, v^*,\, u,\, u^*\right). \tag{5}$$

If the two elements are not identical—for example, if one channel is dissipative while the other one draws energy from outside—the system may be still invariant under a relaxed form of the left–right permutation known as the parity-time ($\mathcal{PT}$) symmetry [9]. Mathematically, the discrete Schrödinger equation is said to be $\mathcal{PT}$-symmetric if it is invariant under the product of $\mathcal{P}$ and $\mathcal{T}$ transformations. Here the $\mathcal{P}$ operator swaps the two elements around:

$$\mathcal{P}\begin{pmatrix} u \\ v \end{pmatrix} = \begin{pmatrix} v \\ u \end{pmatrix},$$

while the $\mathcal{T}$ represents the effect of time inversion on the complex amplitudes: $\mathcal{T}u(t) = u^*(-t)$, $\mathcal{T}v(t) = v^*(-t)$.

The current upsurge of interest in the $\mathcal{PT}$-symmetric systems is due to the fact that they can strike the balance between the gain of energy in one channel and loss in the other. In the optical context, the $\mathcal{PT}$-symmetric dimer describes a waveguide with power loss coupled to a waveguide experiencing optical gain [2, 3, 10–13]. In the matter-wave setting, the $\mathcal{PT}$-symmetric system is formed by two quantum states, with one state leaking and the other one being fed with particles [14, 15].

Since the $\mathcal{PT}$-symmetric systems have channels for the energy exchange with the environment, they are commonly thought to occupy a niche between dissipative and conservative systems. It was therefore met with surprise when some linear [16] and nonlinear [17] $\mathcal{PT}$-symmetric systems were found to possess Hamiltonian structure. In particular, there are Hamiltonian $\mathcal{PT}$-symmetric dimers; one example was produced in [17]:

$$\begin{aligned} \mathrm{i}\dot{u} + v + \left(|u|^2 + 2\,|v|^2\right)u + v^2u^* &= \quad \mathrm{i}\gamma u, \\ \mathrm{i}\dot{v} + u + \left(|v|^2 + 2\,|u|^2\right)v + u^2v^* &= -\,\mathrm{i}\gamma v. \end{aligned} \tag{6}$$

The two terms in the right-hand sides of (6) account for the gain and loss of energy, with $\gamma > 0$ being the gain–loss coefficient.

Another Hamiltonian $\mathcal{PT}$-symmetric system was identified in [18]:

$$\begin{aligned} \mathrm{i}\dot{u} + v + |u|^2u &= \quad \mathrm{i}\gamma u, \\ \mathrm{i}\dot{v} + u + |v|^2v &= -\,\mathrm{i}\gamma v. \end{aligned} \tag{7}$$

Because of its ubiquity in physics [2, 3, 12–14, 19], equation (7) is occasionally referred to as the *standard* dimer.

Finally, the Hamiltonian model

$$\begin{aligned} \mathrm{i}\dot{u} + v - \left(2\alpha_1 + \alpha_2\right)|u|^2v - 2\alpha_1\,|v|^2v &= \quad \mathrm{i}\gamma u, \\ \mathrm{i}\dot{v} + u - \left(2\alpha_1 + \alpha_2\right)|v|^2u - 2\alpha_1\,|u|^2u &= -\,\mathrm{i}\gamma v, \end{aligned} \tag{8}$$

was discovered outside the domain of the $\mathcal{PT}$-symmetry—as a by-product in the search of integrable equation [20]. Here $\alpha_1$ and $\alpha_2$ are arbitrary real coefficients.

The availability of the Hamiltonian structure is a fundamental property of a dynamical system. This property by itself implies the conservation of phase volume and hence some degree of regularity of motion. But in the presence of additional first integrals it allows to establish an even higher level of regularity, namely, the Liouville integrability.

The first aim of this paper is to show that *any* cubic $\mathcal{PT}$-symmetric phase-invariant dimer obtained as a $\mathcal{PT}$-symmetric extension of the conservative dimer (3) or (4), is a Hamiltonian

system. By determining an additional integral of motion independent of the Hamiltonian, we establish the complete integrability of all these systems.

Another topic pursued in the present study concerns the phenomenon of $\mathcal{PT}$-symmetry breaking—one of the experimentally accessible properties of physical systems with gain and loss [12, 21–23]. The spontaneous symmetry breaking occurs in *linear* $\mathcal{PT}$-symmetric systems as the gain–loss coefficient is increased beyond a critical value $\gamma_c$. This exceptional point separates the symmetric phase ($\gamma < \gamma_c$), where all perturbation frequencies are real, and the symmetry-broken phase ($\gamma > \gamma_c$), where some frequencies are complex and the corresponding modes grow exponentially.

When the input power in the physical structure is low—or, equivalently, when the initial conditions of the corresponding mathematical model are small—all nonlinear effects are negligible and the system follows the linear laws. In particular, small initial conditions in the symmetry-broken phase trigger an exponential growth. However as the resulting solution reaches finite amplitude, the nonlinear coupling terms kick in. These terms may channel the power from the site where it is gained, to the site where it is lost. The higher is the power gained, the larger portion of it is channeled to the disposal site by the nonlinear coupling. In systems where this mechanism is at work, the exponential growth is arrested and all escaping trajectories are sent back to the finite part of the phase space. The $\mathcal{PT}$ symmetry becomes spontaneously restored.

The classification of integrable $\mathcal{PT}$-symmetric dimers with the nonlinearly restored $\mathcal{PT}$-symmetry, is the second objective of our study.

The outline of the paper is as follows.

In section 2 we present a four-parameter family of the $\mathcal{PT}$-symmetric *cross-gradient* dimers; all these systems are Hamiltonian in their original $u$ and $v$ variables. In a similar way, a four-parameter $\mathcal{PT}$-symmetric extension of the *straight-gradient* dimer is introduced in section 3.

The straight-gradient systems do not admit the Hamiltonian formulation in terms of $u$ and $v$—except when the straight-gradient system is cross-gradient at the same time, or when it is gauge-equivalent to a cross-gradient system. (We identify such dual cases in section 3.) Nevertheless, transforming to the Stokes variables (section 4) we can describe all trajectories of the straight-gradient dimer and elucidate the geometry of its phase space.

In the subsequent three sections we determine the canonical coordinates for the general straight-gradient dimer and reformulate it as a Hamiltonian system. Three complementary subfamilies of the straight-gradient models are considered (sections 5, 6 and 7).

Section 8 is concerned with the trajectory confinement and $\mathcal{PT}$-symmetry restoration. We identify broad classes of nonlinearities capable of suppressing the exponential blowup regimes—both within the cross-gradient and straight-gradient families.

Section 9 offers examples of simple oscillatory systems with the amplitude equations in the form of cross- and straight-gradient dimers.

Finally, in section 10 we summarize mathematical results of this study and discuss their physical implications.

## 2. Cross-gradient $\mathcal{PT}$-symmetric dimer

A general cross-gradient dimer (4), complying with the phase invariance (2), with no gain or loss, with cubic nonlinearity, permutation property (5) and linear part of the form (1), is defined by the Hamiltonian

$$\mathfrak{H}_0 = -\big(|u|^2 + |v|^2\big) + W(u, v). \tag{9}$$

Here $W$ is a $U(1)$-invariant real quartic polynomial in $u$, $v$ and their complex-conjugates, which is symmetric with respect to the $u \leftrightarrows v$ permutations. The most general quartic polynomial with these properties can be written as

$$W = \alpha_1\big(|u|^2 + |v|^2\big)^2 + \alpha_2\,|u|^2|v|^2 + \alpha_3\big(u^*v + uv^*\big)\big(|u|^2 + |v|^2\big) + \alpha_4\big(u^*v + uv^*\big)^2, \tag{10}$$

where $\alpha_1$, $\alpha_2$, $\alpha_3$, and $\alpha_4$ are real coefficients. (See section 2 in [24].)

For any set of $\alpha$'s, this gainless lossless system admits a straightforward $\mathcal{PT}$-symmetric extension

$$\mathrm{i}\frac{\mathrm{d}u}{\mathrm{d}t} = \frac{\partial\mathfrak{H}}{\partial v^*}, \qquad \mathrm{i}\frac{\mathrm{d}v}{\mathrm{d}t} = \frac{\partial\mathfrak{H}}{\partial u^*}, \tag{11}$$

where the Hamilton function $\mathfrak{H}$ is different from $\mathfrak{H}_0$ in just one term:

$$\mathfrak{H} = -\big(|u|^2 + |v|^2\big) + W(u, v) + \mathrm{i}\gamma\big(uv^* - u^*v\big). \tag{12}$$

Here $\gamma > 0$ is the gain–loss coefficient. Substituting the expression (12) with $W$ as in (10) in equation (11), we obtain a four-parameter family of Hamiltonian $\mathcal{PT}$-symmetric cubic dimers:

$$\begin{aligned}
\mathrm{i}\dot u + v - \mathrm{i}\gamma u &= \alpha_3\big(|u|^2 + 2\,|v|^2\big)u + \alpha_3 v^2u^* + 2\alpha_4u^2v^* \\
&\quad + \Big[\big(2\alpha_1 + \alpha_2 + 2\alpha_4\big)\,|u|^2 + 2\alpha_1\,|v|^2\Big]v, \\
\mathrm{i}\dot v + u + \mathrm{i}\gamma v &= \alpha_3\big(2\,|u|^2 + |v|^2\big)v + \alpha_3u^2v^* + 2\alpha_4v^2u^* \\
&\quad + \Big[\big(2\alpha_1 + \alpha_2 + 2\alpha_4\big)\,|v|^2 + 2\alpha_1\,|u|^2\Big]u.
\end{aligned} \tag{13}$$

A particular case of (13) is the system (6). This is selected by letting $\alpha_3 = -1$ and $\alpha_1 = \alpha_2 = \alpha_4 = 0$. Another special case is the dimer (8); this model corresponds to $\alpha_3 = \alpha_4 = 0$. The Hamiltonian structure of these two particular systems has been determined earlier [17, 20].

Despite the seeming complexity, all trajectories of (13) admit a simple analytic description. We define the Stokes vector $\boldsymbol{\mathcal{R}} = \mathbf{i}X + \mathbf{j}Y + \mathbf{k}Z$, where

$$X = u^*v + v^*u, \qquad Y = \mathrm{i}\big(u^*v - v^*u\big), \qquad Z = |u|^2 - |v|^2. \tag{14}$$

Note that the length $\mathcal{R} = \sqrt{X^2 + Y^2 + Z^2}$ of the Stokes vector has a simple expression in terms of $u$ and $v$:

$$\mathcal{R} = |u|^2 + |v|^2.$$

Transforming to $X$, $Y$, and $Z$, equations (13) give a dynamical system in three dimensions:

$$\dot X = 0, \tag{15a}$$

$$\dot Y = -2Z + 2\alpha_3XZ + 4\alpha_1Z\mathcal{R}, \tag{15b}$$

$$\dot Z = 2Y + 2\gamma\mathcal{R} - 2\alpha_3XY - \big(\alpha_2 + 4\alpha_1\big)Y\mathcal{R}. \tag{15c}$$

Equation (15*a*) implies that for any selection of $\alpha_1$, $\alpha_2$, $\alpha_3$, and $\alpha_4$, the cross-gradient dimer (13) has two independent integrals of motion: $X$ and $\mathfrak{H}$. Accordingly, the Hamiltonian system (13) is Liouville-integrable.

All trajectories lie in parallel vertical planes $X = X_0$, where $X_0$ is an arbitrary constant. The form of the trajectories is determined by setting $X = X_0$ in the equation

$\mathfrak{H}(X, Y, Z) = const$, with $\mathfrak{H}$ being the Hamiltonian (12) expressed in the Stokes variables:

$$Y\left(\frac{\alpha_2}{4}Y - \gamma\right) + \mathcal{R}\left(\alpha_1\mathcal{R} + \alpha_3 X_0 - 1\right) = C. \tag{16}$$

Here $C$ is a constant of integration. Equation (16) with $\mathcal{R} = \sqrt{X_0^2 + Y^2 + Z^2}$ defines a one-parameter family of trajectories on the $X = X_0$ plane.

## 3. Straight-gradient $\mathcal{PT}$-symmetric dimer

The conservative straight-gradient dimer with general cubic nonlinearity, left–right symmetry and phase invariance, has the form

$$\mathrm{i}\frac{\mathrm{d}u}{\mathrm{d}t} = \frac{\partial\mathcal{H}}{\partial u^*}, \qquad \mathrm{i}\frac{\mathrm{d}v}{\mathrm{d}t} = \frac{\partial\mathcal{H}}{\partial v^*}, \tag{17}$$

where

$$\mathcal{H} = -\left(uv^* + u^*v\right) + W(u, v), \tag{18}$$

and $W$ is the four-parameter quartic polynomial:

$$W = \beta_1\left(|u|^2 + |v|^2\right)^2 + \beta_2\,|u|^2|v|^2 + \beta_3\left(u^*v + uv^*\right)\left(|u|^2 + |v|^2\right) + \beta_4\left(u^*v + uv^*\right)^2. \tag{19}$$

Here $\beta_1$, $\beta_2$, $\beta_3$, and $\beta_4$ are real coefficients. This is the same quartic as in the previous section; we have just switched from the $\alpha$- to the $\beta$-notation to emphasise that we consider a totally new family of models.

The system (17)–(19) with $\beta_1 = -\frac{1}{2}$, $\beta_2 = 1$, and $\beta_3 = \beta_4 = 0$ is known as the $N = 2$ discrete self-trapping equation [6]. When $\beta_3 = \beta_4 = 0$ while $\beta_1 = -\rho/2$, $\beta_2 = \rho - 1$ with $\rho$ a real coefficient, these equations constitute the spatially homogeneous version of the Aceves-Wabnitz coupled mode system for the nonlinear optical grating [25]. A particular case of this ($\beta_1 = 0$, $\beta_2 = -1$) is the spatially-independent Thirring model (a theory of self-interacting spinor field) [26–28]. Another case related to spinors is $\beta_4 = -\frac{1}{2}$, $\beta_1 = \beta_2 = \beta_3 = 0$; this system derives from the one-component Gross–Neveu model [27, 29]. The system with $\beta_2 = 2$, $\beta_4 = -\frac{1}{2}$, $\beta_1 = \beta_3 = 0$ is related to the spinor theory with the pseudoscalar interaction [28, 30].

The $\mathcal{PT}$-symmetric extension of the general straight-gradient dimer (17) has the form

$$\mathrm{i}\frac{\mathrm{d}u}{\mathrm{d}t} - \mathrm{i}\gamma u = \frac{\partial\mathcal{H}}{\partial u^*}, \qquad \mathrm{i}\frac{\mathrm{d}v}{\mathrm{d}t} + \mathrm{i}\gamma v = \frac{\partial\mathcal{H}}{\partial v^*}. \tag{20}$$

Evaluating the partial derivatives using (18) and (19), these equations become

$$\begin{aligned}
\mathrm{i}\dot{u} + v - \mathrm{i}\gamma u &= \left[2\beta_1\,|u|^2 + \left(2\beta_1 + \beta_2 + 2\beta_4\right)|v|^2\right]u \\
&\quad + 2\beta_4 v^2u^* + \beta_3u^2v^* + \beta_3\left(2\,|u|^2 + |v|^2\right)v, \\
\mathrm{i}\dot{v} + u + \mathrm{i}\gamma v &= \left[2\beta_1\,|v|^2 + \left(2\beta_1 + \beta_2 + 2\beta_4\right)|u|^2\right]v \\
&\quad + 2\beta_4u^2v^* + \beta_3v^2u^* + \beta_3\left(2\,|v|^2 + |u|^2\right)u.
\end{aligned} \tag{21}$$

The *standard* dimer (7) is a special case of (21). This is selected by taking $\beta_1 = -\frac{1}{2}$, $\beta_2 = 1$, and $\beta_3 = \beta_4 = 0$ in equation (21). There is an extensive literature on mathematical aspects of this model [13, 18, 31–37].

The couples $(u,\ u^*)$ and $(v,\ v^*)$ do not form pairs of canonically conjugate variables. That is, the straight-gradient dimer (21) does not admit a Hamiltonian formulation in terms of the original complex coordinates—except when the straight-gradient dimer is cross-gradient at the same time. The necessary and sufficient condition for the equation (17) to have a representation (11) with some $\mathfrak{H}$, is

$$\frac{\partial}{\partial u^*}\left(\mathrm{i}\gamma u + \frac{\partial \mathcal{H}}{\partial u^*}\right) = \frac{\partial}{\partial v^*}\left(-\mathrm{i}\gamma v + \frac{\partial \mathcal{H}}{\partial v^*}\right).$$

For $\mathcal{H}$ of the form (18), this condition translates into

$$\frac{\partial^2 W}{\partial u^{*2}} = \frac{\partial^2 W}{\partial v^{*2}}.$$

Substituting the quartic polynomial (19) for $W$ gives, finally, $\beta_1 = \beta_4$.

The choice $\beta_1 = \beta_4$ ensures the existence of a (complex) function $\mathfrak{H}$ such that

$$\mathrm{i}\gamma u + \frac{\partial \mathcal{H}}{\partial u^*} = \frac{\partial \mathfrak{H}}{\partial v^*}, \quad -\mathrm{i}\gamma u^* + \frac{\partial \mathcal{H}}{\partial u} = \frac{\partial \mathfrak{H}^*}{\partial v}, \tag{22}$$

$$-\mathrm{i}\gamma v + \frac{\partial \mathcal{H}}{\partial v^*} = \frac{\partial \mathfrak{H}}{\partial u^*}, \quad \mathrm{i}\gamma v^* + \frac{\partial \mathcal{H}}{\partial v} = \frac{\partial \mathfrak{H}^*}{\partial u}. \tag{23}$$

The necessary and sufficient condition for the function $\mathfrak{H}$ in (22) to be real, is given by

$$\frac{\partial}{\partial v}\left(\mathrm{i}\gamma u + \frac{\partial \mathcal{H}}{\partial u^*}\right) = \frac{\partial}{\partial v^*}\left(-\mathrm{i}\gamma u^* + \frac{\partial \mathcal{H}}{\partial u}\right).$$

In a similar way, the necessary and sufficient condition for $\mathfrak{H} = \mathfrak{H}^*$ in equation (23) is

$$\frac{\partial}{\partial u}\left(-\mathrm{i}\gamma v + \frac{\partial \mathcal{H}}{\partial v^*}\right) = \frac{\partial}{\partial u^*}\left(\mathrm{i}\gamma v^* + \frac{\partial \mathcal{H}}{\partial v}\right).$$

For $\mathcal{H}$ of the form (18), each of these two conditions amounts to

$$\frac{\partial^2 W}{\partial v^* \partial u} = \frac{\partial^2 W}{\partial u^* \partial v},$$

which gives $2\beta_1 + \beta_2 = 2\beta_4$. Using the previously established condition $\beta_1 = \beta_4$, this relation reduces simply to $\beta_2 = 0$.

Thus, the straight-gradient dimer (21) with $\beta_1 = \beta_4$ and $\beta_2 = 0$ is, at the same time, a Hamiltonian system with the cross-gradient canonical structure (11). The corresponding Hamilton function $\mathfrak{H}$ is determined by simple integration:

$$\begin{aligned}\mathfrak{H} = &-\left(|u|^2 + |v|^2\right) + \frac{\beta_3}{2}\left(|u|^2 + |v|^2\right)^2 + 2\beta_4\left(|u|^2 + |v|^2\right)\left(uv^* + u^*v\right)\\ &+ \frac{\beta_3}{2}\left(uv^* + vu^*\right)^2 + \mathrm{i}\gamma\left(uv^* - vu^*\right).\end{aligned} \tag{24}$$

The cross-gradient Hamiltonian (24) is of the form (12), (10) with $\alpha_1 = \alpha_4 = \frac{1}{2}\beta_3$, $\alpha_2 = 0$, and $\alpha_3 = 2\beta_4$.

In fact, the class of straight-gradient dimers admitting the Hamiltonian formulation is even wider. Let $u_0$ and $v_0$ be a solution to the straight-gradient equation (21) with $\beta_2 = 0$ and *generic* $\beta_1$, $\beta_4$ (that is, $\beta_1$ not necessarily coinciding with $\beta_4$). The gauge transformation

$$u_0 = \mathrm{e}^{\mathrm{i}\varphi}u, \quad v_0 = \mathrm{e}^{\mathrm{i}\varphi}v$$

with

$$\varphi(t) = 2\big(\beta_4 - \beta_1\big)\int_0^t \big(|u|^2 + |v|^2\big)\mathrm{d}\tau$$

generates functions $u$ and $v$ which satisfy the straight-gradient dimer equations with $\beta_2 = 0$ and $\beta_1$ set equal to $\beta_4$:

$$\begin{aligned}
&\mathrm{i}\dot{u} + v - \mathrm{i}\gamma u = 2\beta_4\big(|u|^2 + 2\,|v|^2\big)u + 2\beta_4 v^2 u^* + \beta_3 u^2 v^* + \beta_3\big(2\,|u|^2 + |v|^2\big)v,\\
&\mathrm{i}\dot{v} + u + \mathrm{i}\gamma v = 2\beta_4\big(|v|^2 + 2\,|u|^2\big)v + 2\beta_4 u^2 v^* + \beta_3 v^2 u^* + \beta_3\big(2\,|v|^2 + |u|^2\big)u.
\end{aligned} \tag{25}$$

As we already know, this system has a cross-gradient Hamiltonian formulation with the Hamilton function (24). Therefore, the straight-gradient dimer with $\beta_2 = 0$ *and any value* of $(\beta_4 - \beta_1)$ is gauge-equivalent to the cross-gradient Hamiltonian system (11), where the Hamilton function $\mathfrak{H}$ is as in (24).

In what follows, we uncover the Hamiltonian formulation of the straight-gradient system (21) with $\beta_2 \neq 0$. This class will include, in particular, the standard dimer (7) (which has $\beta_2 = 1$).

## 4. Phase space of straight-gradient dimer

The generic ($\beta_2 \neq 0$) straight-gradient dimer does not admit the Hamiltonian formulation in terms of the original $u$ and $v$ variables. In order to determine the canonical pairs of coordinates, we transform it to the Stokes variables (14). Equations (21) give a dynamical system in three-dimensions:

$$\dot{X} = -\beta_2 YZ, \tag{26a}$$

$$\dot{Y} = -2Z + \big(\beta_2 + 4\beta_4\big)XZ + 2\beta_3 Z\mathcal{R}, \tag{26b}$$

$$\dot{Z} = 2Y + 2\gamma\mathcal{R} - 4\beta_4 XY - 2\beta_3\mathcal{R}Y. \tag{26c}$$

We also note an equation for the length of the Stokes vector that follows from the system (26):

$$\dot{\mathcal{R}} = 2\gamma Z. \tag{27}$$

Replacing $t$ with $\mathcal{R}$ as a new independent variable, and using $\mathrm{d}/\mathrm{d}t = \dot{\mathcal{R}}\,\mathrm{d}/\mathrm{d}\mathcal{R}$, equations (26*a*) and (26*b*) become a linear nonhomogeneous system

$$\begin{aligned}
&2\gamma\frac{\mathrm{d}X}{\mathrm{d}\mathcal{R}} + \beta_2 Y = 0,\\
&2\gamma\frac{\mathrm{d}Y}{\mathrm{d}\mathcal{R}} - \big(\beta_2 + 4\beta_4\big)X = -2 + 2\beta_3\mathcal{R}.
\end{aligned} \tag{28}$$

Our strategy will be to determine the general solution of (28) including two constants of integration. These 'constants of motion' of the system (28) will serve as the two first integrals of the original three-dimensional dynamical system (26). To obtain the Hamiltonian formulation of the dimer (21), one of these will be appointed as the Hamiltonian and the other one as a canonical coordinate.

As in the case of the cross-gradient dimer, the existence of two independent conserved quantities along with the availability of the Hamiltonian structure will imply that the straight-gradient dimer (21) is Liouville integrable.

It is convenient to introduce the quantity

$$\omega^2 \equiv \beta_2\left(\beta_2 + 4\beta_4\right). \tag{29}$$

The form of the solution of the system (28) depends on whether $\omega^2$ is positive, negative or zero. We consider these three cases separately.

Assuming that $\omega^2 > 0$, the general solution of (28) is

$$X = A\cos\left(\frac{\omega}{2\gamma}\mathcal{R}\right) + B\sin\left(\frac{\omega}{2\gamma}\mathcal{R}\right) + \frac{2 - 2\beta_3\mathcal{R}}{\beta_2 + 4\beta_4}, \tag{30a}$$

$$Y = \frac{\omega}{\beta_2}\left[A\sin\left(\frac{\omega}{2\gamma}\mathcal{R}\right) - B\cos\left(\frac{\omega}{2\gamma}\mathcal{R}\right)\right] + \frac{4\gamma\beta_3}{\omega^2}, \tag{30b}$$

where $A$ and $B$ are constants of integration. Treating $\mathcal{R}$ as a parameter, and supplementing (30*a*)–(30*b*) with the formula

$$Z = \pm\sqrt{\mathcal{R}^2 - X^2(\mathcal{R}) - Y^2(\mathcal{R})}, \tag{30c}$$

these equations provide explicit parametric expressions for trajectories of the dimer: $X = X(\mathcal{R})$, $Y = Y(\mathcal{R})$, $Z = Z(\mathcal{R})$.

Denoting $\rho = \sqrt{A^2 + B^2}$, equations (30*a*) and (30*b*) give

$$\rho^2 = \left(X + \frac{2\beta_3\mathcal{R} - 2}{\beta_2 + 4\beta_4}\right)^2 + \left(\frac{\beta_2}{\omega}\right)^2\left(Y - \frac{4\gamma\beta_3}{\omega^2}\right)^2. \tag{31}$$

Equation (31) with $\mathcal{R} = \sqrt{X^2 + Y^2 + Z^2}$ is an implicit equation of the surface on which all trajectories lie. The shape of this surface in the $(X, Y, Z)$ phase space depends on the value of the parameter

$$\sigma = \frac{2\beta_3}{\beta_2 + 4\beta_4}. \tag{32}$$

Figures 1(a), (b), and (c) depict the surface with $|\sigma| < 1$, $|\sigma| > 1$, and $|\sigma| = 1$.

In the case where $\omega^2 < 0$, we define $\nu^2 = -\omega^2 > 0$. The general solution of (28) is then

$$X = C\exp\left(\frac{\nu}{2\gamma}\mathcal{R}\right) + D\exp\left(-\frac{\nu}{2\gamma}\mathcal{R}\right) + \frac{2 - 2\beta_3\mathcal{R}}{\beta_2 + 4\beta_4}, \tag{33a}$$

$$Y = -\frac{\nu}{\beta_2}\left[C\exp\left(\frac{\nu}{2\gamma}\mathcal{R}\right) - D\exp\left(-\frac{\nu}{2\gamma}\mathcal{R}\right)\right] - \frac{4\gamma\beta_3}{\nu^2}, \tag{33b}$$

where $C$ and $D$ are two constants of integration.

Expressing $4CD$ in terms of $X$, $Y$, $\mathcal{R}$ and denoting it $s_1 s_2\rho^2$, where $s_1 = \operatorname{sign} C$ and $s_2 = \operatorname{sign} D$, we obtain

$$s_1 s_2\rho^2 = \left(X + \sigma\mathcal{R} - \frac{2}{\beta_2 + 4\beta_4}\right)^2 - \left(\frac{\beta_2}{\nu}\right)^2\left(Y + \frac{4\gamma\beta_3}{\nu^2}\right)^2. \tag{34}$$

Here $\rho \geqslant 0$ and $s_1 s_2$ is either 1 or $-1$, depending on whether $CD > 0$ or $CD < 0$. The solution surface (34) made up by all trajectories of the dimer, is shown in figures 1 (d), (e), and (f) for $|\sigma| < 1$, $|\sigma| > 1$, and $|\sigma| = 1$, respectively.

Finally, the case $\omega^2 = 0$ is considered in section 7 below.

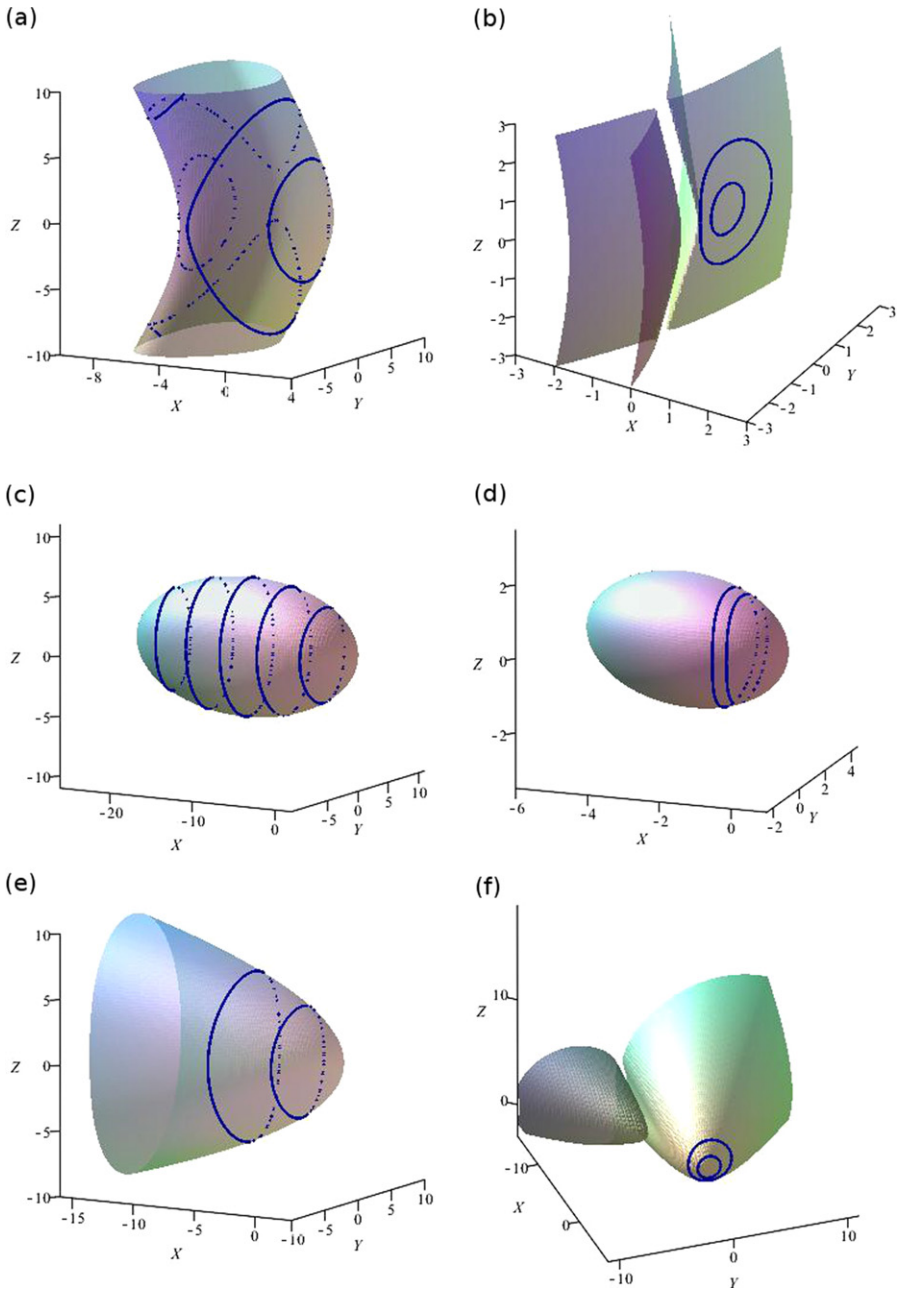


**Figure 1.** The surface (31) with $\omega^2 > 0$ (a), (c), (e) and $\omega^2 < 0$ (b), (d), (f). The parameter $|\sigma|$ is smaller than 1 in (a), (b); greater than 1 in (c), (d), and equal to 1 in (e), (f). The value of $\beta_2$ is 1 in (a), (c), (e) and $-1$ in (b), (d), (f). The value of $\beta_3$ is 2 in (a), 1 in (b), 5 in (c), 9/2 in (d), (e), and 7/2 in (f). In all panels, $\gamma = 1$ and $\beta_4 = 2$. The surface parameter $\rho^2 = 7$ in (a), (c), (e) and $s_1 s_2 \rho^2 = -\frac{1}{100}$ in (b), (d), (f). We also show a few trajectories of the system (26) lying on each surface.

## 5. Hamiltonian structure of straight-gradient dimer: $\omega^2 > 0$

It is convenient to write the explicit solution (30*a*)–(30*b*) in the complex form

$$X + \mathrm{i}\frac{\beta_2}{\omega}Y = \rho \mathrm{e}^{-\mathrm{i}\theta} + \frac{2 - 2\beta_3\mathcal{R}}{\beta_2 + 4\beta_4} + \mathrm{i}\frac{4\gamma\beta_2\beta_3}{\omega^3}, \tag{35}$$

where

$$\rho \mathrm{e}^{-\mathrm{i}\theta} = (A - \mathrm{i}B)\exp\left(\mathrm{i}\frac{\omega}{2\gamma}\mathcal{R}\right) \tag{36}$$

and $\rho = \sqrt{A^2 + B^2}$ was introduced in the previous section. Assume $\rho > 0$; in this case, equation (36) serves as the definition of $\theta$. (We will examine the possibility $\rho = 0$ in subsection 5.4 below.) Using equation (35), $\theta$ is expressible as a function of $X$, $Y$, and $\mathcal{R}$:

$$\theta = \arctan\left(\frac{\omega}{\beta_2}\frac{X + \sigma\mathcal{R} - 2\beta_2\omega^{-2}}{Y - 4\gamma\beta_3\omega^{-2}}\right). \tag{37}$$

The definition (36) implies that the complex quantity

$$\rho \exp\left\{\frac{\mathrm{i}}{2\gamma}(-2\gamma\theta - \omega\mathcal{R})\right\} = A - \mathrm{i}B$$

is a constant. Therefore its argument

$$H = -2\gamma\theta - \omega\mathcal{R} \tag{38}$$

is a first integral of the system (26). We shall demonstrate that $H$ can serve as a Hamilton function for the three-dimensional system (26) and the underlying nonlinear Schrödinger dimer (21).

One more integral of motion, $\rho$, is given by (31). Choosing $\rho$ and $\theta$ as a pair of coordinates in the phase space, we require that $\mathcal{R}$ (and hence $H$) be a function of $\rho$, $\theta$, and $P_\theta$—but not depend on $P_\rho$ [18]. Irrespectively of how we define $P_\rho$, the Hamilton equation

$$\dot{\rho} = \frac{\partial H}{\partial P_\rho} \tag{39}$$

will then reproduce the equation for $\rho$: $\dot{\rho} = 0$. Another consequence of requiring $\partial H/\partial P_\rho = 0$, is that the variable $P_\rho$ will not participate in the dynamics and the Hamilton equation

$$\dot{P}_\rho = -\frac{\partial H}{\partial \rho} \tag{40}$$

will decouple from the rest of the system.

At this point, we note that, since $\theta$ is only different from $-\frac{\omega}{2\gamma}\mathcal{R}$ by a constant, equation (27) gives

$$\dot{\theta} = -\omega Z. \tag{41}$$

We should choose the momentum $P_\theta$ (denoted $\mathcal{P}$ for brevity) in such a way that the canonical equation

$$\dot{\theta} = \frac{\partial H}{\partial \mathcal{P}} \tag{42}$$

reproduces equation (41). For the Hamilton function of the form (38), equations (42) and (41) are equivalent if

$$\frac{\partial \mathcal{R}}{\partial \mathcal{P}} = Z. \tag{43}$$

Once the equation (42) is satisfied, the conjugate equation

$$\dot{\mathcal{P}} = -\frac{\partial H}{\partial \theta} \tag{44}$$

will be verified automatically. Indeed, since $H$ does not depend on $P_\rho$ while $\dot{\rho} = 0$, there are only two nonvanishing terms in the derivative $\dot{H}$:

$$\dot{H} = \frac{\partial H}{\partial \theta}\dot{\theta} + \frac{\partial H}{\partial \mathcal{P}}\dot{\mathcal{P}}.$$

Substituting for $\dot{\theta}$ from (42), the relation $\dot{H} = 0$ implies equation (44).

Thus all we need to do in order to put the canonical structure in place, is to identify the canonical momentum $\mathcal{P} = P_\theta$ ensuring the validity of equation (43). Before proceeding to the unveiling of $P_\theta$, a technical remark is in order. Equation (35) implies that the coordinate $Y$ can be expressed solely in terms of $\rho$ and $\theta$ (rather than $\rho$, $\theta$, and $\mathcal{R}$):

$$Y = \frac{4\gamma\beta_3}{\omega^2} + \frac{\omega}{\beta_2}\rho\cos\theta. \tag{45}$$

Therefore $\theta$ may be thought of as the spherical polar angle in the frame of reference where $Y$ is the vertical coordinate. In what follows, we also introduce (an analogue of) the azimuthal angle on the $(X, Z)$-plane. This construction will be based on the following decomposition of the coordinate $X$ stemming from (35):

$$X = x - \sigma\mathcal{R}. \tag{46}$$

Here we have isolated a term that is expressible entirely in terms of $\rho$ and $\theta$:

$$x = \frac{2}{\beta_2 + 4\beta_4} + \rho\sin\theta. \tag{47}$$

Our construction of the canonical momentum $P_\theta$ depends on whether the parameter $\sigma$ defined in (32) is smaller, greater, or equal to 1 in magnitude.

### *5.1. Hyperbolic case:* $|\sigma| < 1$

Assuming $|\sigma| < 1$, we define

$$\Lambda^2 = 1 - \sigma^2 > 0.$$

The corresponding subfamily of models includes, in particular, the standard dimer (7)—for which $\omega^2 = 1$ and $\sigma = 0$. (We note that the Hamiltonian structure of the standard dimer was elucidated earlier [18].)

Inserting the decomposition (46) in the identity $X^2 + Y^2 + Z^2 = \mathcal{R}^2$ yields

$$\left(\Lambda\mathcal{R} + \frac{\sigma}{\Lambda}x\right)^2 - \left(\frac{\partial \mathcal{R}}{\partial \mathcal{P}}\right)^2 = r^2, \tag{48}$$

where we have substituted for $Z$ from (43) and defined

$$r^2 = \frac{x^2}{\Lambda^2} + Y^2. \tag{49}$$

Since $x$ and $r$ are expressible in terms of $\rho$ and $\theta$ only (i.e., are independent of $\mathcal{P}$), equation (48) is an ordinary differential equation for $\mathcal{R}(\mathcal{P})$. To define $\mathcal{P}$, it is sufficient to pick one solution of this separable equation. We choose

$$\mathcal{R}(\mathcal{P}) = \frac{r}{\Lambda}\cosh(\Lambda\mathcal{P}) - \frac{\sigma}{\Lambda^2}x; \tag{50}$$

the formula (43) gives then

$$Z = r\sinh(\Lambda\mathcal{P}), \tag{51}$$

so that

$$P_\theta = \mathcal{P} = \frac{1}{\Lambda}\text{arcsinh}\left(\frac{Z}{r}\right). \tag{52}$$

Together with the definition of the coordinate $\rho$ in (31), the coordinate $\theta$ in (37), the definition (52) completes the set of three canonical variables. The fourth coordinate, $P_\rho$, can be reconstructed from equation (40) by the integration of its right-hand side in $t$.

Summarizing, we have cast the straight-gradient dimer (21) with $\omega^2 > 0$ and $\sigma^2 < 1$ in the form of a Hamiltonian system

$$\dot\rho = \frac{\partial H}{\partial P_\rho}, \quad \dot P_\rho = -\frac{\partial H}{\partial \rho}, \quad \dot\theta = \frac{\partial H}{\partial P_\theta}, \quad \dot P_\theta = -\frac{\partial H}{\partial \theta}, \tag{53}$$

with the Hamilton function

$$H(\rho, \theta, P_\theta) = -2\gamma\theta - \frac{\omega}{\Lambda^2}\left[\Lambda r\cosh(\Lambda P_\theta) - \sigma x\right].$$

Here $x = x(\rho, \theta)$ and $r = r(\rho, \theta)$ are as in (47) and (49), respectively; the variable $Y$ in (49) is defined in (45).

### 5.2. Elliptic case: $|\sigma| > 1$

Assuming that $\sigma^2 > 1$ and defining

$$\Omega^2 = \sigma^2 - 1 > 0,$$

the identity $X^2 + Y^2 + Z^2 = \mathcal{R}^2$ becomes an ordinary differential equation for $\mathcal{R}(\mathcal{P})$:

$$\left(\Omega\mathcal{R} - \frac{\sigma}{\Omega}x\right)^2 + \left(\frac{\partial\mathcal{R}}{\partial\mathcal{P}}\right)^2 = r^2. \tag{54}$$

Here we used (43), while the variable $r$ was introduced differently from (49):

$$r^2 = \frac{x^2}{\Omega^2} - Y^2.$$

The separable equation (54) is solved by taking

$$\mathcal{R} = -\frac{r}{\Omega}\cos(\Omega\mathcal{P}) + \frac{\sigma}{\Omega^2}x; \tag{55}$$

hence $Z = r\,\sin(\Omega\mathcal{P})$. This provides a simple expression for the canonical momentum:

$$P_\theta = \mathcal{P} = \Omega^{-1}\arcsin(Z/r) \tag{56}$$

Thus, the straight-gradient dimer (21) with $\omega^2 > 0$ and $\sigma^2 > 1$ is cast in the form (53) with

$$H\big(\rho,\,\theta,\,P_\theta\big) = -2\gamma\theta + \frac{\omega}{\Omega^2}\Big[\,\Omega r\,\cos\big(\Omega P_\theta\big) - \sigma x\Big],$$

where $x = x\,(\rho,\,\theta)$ and $r = r\,(\rho,\,\theta)$.

### 5.3. Parabolic case: $|\sigma| = 1$

Assuming $\sigma = \pm 1$, the identity $X^2 + Y^2 + Z^2 = \mathcal{R}^2$ reduces to an equation

$$x^2 + Y^2 + \left(\frac{\partial\mathcal{R}}{\partial\mathcal{P}}\right)^2 = 2\sigma x\mathcal{R}, \tag{57}$$

with a solution

$$\mathcal{R} = \frac{\sigma}{2}x\left(\mathcal{P}^2 + 1 + \frac{Y^2}{x^2}\right). \tag{58}$$

The rule (43) gives then $Z = \sigma x\mathcal{P}$, so that

$$\mathcal{P} = \sigma\frac{Z}{x}. \tag{59}$$

The construction of the canonical variables in the $\sigma = \pm 1$ sector is hereby complete. In the canonical equation (53), the Hamiltonian is

$$H\big(\rho,\,\theta,\,P_\theta\big) = -2\gamma\theta - \frac{\omega\sigma x}{2}\left[\,P_\theta^2 + 1 + \frac{Y^2}{x^2}\right],$$

with $x = x\,(\rho,\,\theta)$ and $Y = Y\,(\rho,\,\theta)$.

### 5.4. One-dimensional motion: $\rho = 0$

Finally, we consider the situation where $A = B = 0$ in (30*a*)–(30*b*) and hence, $\rho = 0$. Equation (31) gives

$$X = \frac{2}{\beta_2 + 4\beta_4} - \sigma\mathcal{R}, \tag{60}$$

$$Y = \frac{4\gamma\beta_3}{\omega^2}. \tag{61}$$

The invariant manifold defined by $\rho = 0$, consists of a single curve lying in the plane (61). The parametric equations for this quadratic curve, with $\mathcal{R}$ as the parameter, are given by (60), (61) and (30*c*).

Using the identity $X^2 + Y^2 + Z^2 = \mathcal{R}^2$, the conserved quantity $-2\gamma^2Y^2$ can be represented as a function of $X$, $Z$ and $\mathcal{R}$:

$$-2\gamma^2Y^2 = 2\gamma^2\big(X^2 + Z^2\big) - 2\gamma^2\mathcal{R}^2. \tag{62}$$

Here $X$ is expressible in terms of $\mathcal{R}$ using (60) and the coefficient $-2\gamma^2$ was introduced for the later convenience.

We choose (62) as Hamilton's function and $\mathcal{R}$ as the canonical coordinate. The only term in (62) that remains independent of $\mathcal{R}$, is $2\gamma^2 Z^2$. Defining the momentum by $\mathcal{P} = 2\gamma Z$, the Hamilton's function (62) becomes

$$H = \frac{\mathcal{P}^2}{2} + U(\mathcal{R}), \quad U = 2\gamma^2\left(\frac{2}{\beta_2 + 4\beta_4} - \sigma\mathcal{R}\right)^2 - 2\gamma^2\mathcal{R}^2, \tag{63}$$

while the canonical equation $\dot{\mathcal{R}} = \partial H/\partial\mathcal{P}$ reproduces equation (27). The conjugate equation $\dot{\mathcal{P}} = -\partial H/\partial\mathcal{R}$ is then satisfied automatically, because of $\dot{H} = 0$.

Thus, the motion along the quadratic curve $\rho = 0$ is governed by a Hamiltonian system with one degree of freedom.

## 6. Hamiltonian structure of straight-gradient dimer: $\omega^2 < 0$

### *6.1. $\rho > 0$: two-dimensional motion*

Turning to the dimers with $\omega^2 < 0$, we continue to employ the first integral $\rho$ as one of the two canonical variables. This time, $\rho^2$ is defined by (34) and equals $4\,|CD|$. Using the explicit solution (33), one can form linear combinations

$$\begin{aligned} X + \frac{\beta_2}{\nu}Y &= s_2\rho e^{-\theta} + \frac{2 - 2\beta_3\mathcal{R}}{\beta_2 + 4\beta_4} - \frac{4\gamma\beta_2\beta_3}{\nu^3}, \\ X - \frac{\beta_2}{\nu}Y &= s_1\rho e^{\theta} + \frac{2 - 2\beta_3\mathcal{R}}{\beta_2 + 4\beta_4} + \frac{4\gamma\beta_2\beta_3}{\nu^3}, \end{aligned} \tag{64}$$

where we have introduced

$$s_1\rho e^{\theta} = 2C\,\exp\left(\frac{\nu}{2\gamma}\mathcal{R}\right), \quad s_2\rho e^{-\theta} = 2D\,\exp\left(\frac{\nu}{2\gamma}\mathcal{R}\right). \tag{65}$$

Provided $\rho > 0$, either of these two equations defines a real $\theta$ which we adopt as the second canonical variable.

Writing equations (65) in the form

$$s_1\frac{2C}{\rho} = \exp\left(\frac{2\gamma\theta - \nu\mathcal{R}}{2\gamma}\right), \quad s_2\frac{2D}{\rho} = \exp\left(\frac{\nu\mathcal{R} - 2\gamma\theta}{2\gamma}\right), \tag{66}$$

we note that since $C$, $D$, and $\rho$ are time-independent, the argument of the exponentials in (66) is a conserved quantity. Therefore

$$H = -2\gamma\theta + \nu\mathcal{R} \tag{67}$$

provides us with the second integral of motion for the system (26*a*). We will employ $H$ as its Hamilton function.

Proceeding to the construction of the momentum $P_\theta = \mathcal{P}$ canonically conjugate to $\theta$, we note that the constancy of the difference $\nu\mathcal{R} - 2\gamma\theta$ together with the equation (27) yield $\dot{\theta} = \nu Z$. Comparing this to the canonical equation (42), we conclude that the variable $\mathcal{P}$ should be introduced so as to satisfy the rule (43)—as in section 5 where we considered the case $\omega^2 > 0$.

When $\omega^2$ was considered positive, the rule (43), the decomposition (46), and the identity $X^2 + Y^2 + Z^2 = \mathcal{R}^2$ were the only relations necessary to derive the representations (52), (56), and (59) for the momentum $\mathcal{P}$. Also used was the fact that $x$ and $Y$ were $\mathcal{P}$-independent. When $\omega^2$ is taken to be negative, equations (64) give

$$Y = \frac{\nu}{\beta_2}\frac{s_2 e^{-\theta} - s_1 e^{\theta}}{2}\rho - \frac{4\gamma\beta_3}{\nu^2};$$

that is, $Y$ remains to be $\mathcal{P}$-independent. As for the $x$, we define it by

$$x = \frac{2}{\beta_2 + 4\beta_4} + \frac{s_1 e^{\theta} + s_2 e^{-\theta}}{2}\rho$$

instead of (47). This preserves the validity of the decomposition (46)—and therefore, of the representations (52), (56), and (59) for the momentum $P_\theta$. As in the case $\omega^2 > 0$, equations (52), (56) and (59) pertain to $|\sigma|$ smaller, greater and equal to 1, respectively.

This completes the Hamiltonian formulation of the ($\omega^2 < 0$)-straight gradient dimer in the part of the phase space with $\rho > 0$. As in the case of the ($\omega^2 > 0$)-subfamily, the canonical equations are given by (53).

### 6.2. $\rho = 0$: *one-dimensional motion*

It remains to consider the invariant manifold $\rho = 0$. The manifold is described by equation (33) with $C = 0$ or $D = 0$ (supplemented by (30*c*) for the vertical coordinate). Assume, for definiteness, that $D = 0$. Then $C$ and $\mathcal{R}$ define a pair of curvilinear coordinates on the manifold—which is, therefore, a two-dimensional surface. We will show that the coordinate curve corresponding to each particular value of $C$, is a trajectory of a Hamiltonian system with one degree of freedom.

Letting $D = 0$, equation (33) become

$$X = C\exp\left(\frac{\nu}{2\gamma}\mathcal{R}\right) + \frac{2 - 2\beta_3\mathcal{R}}{\beta_2 + 4\beta_4}, \qquad Y = -\frac{\nu}{\beta_2}C\exp\left(\frac{\nu}{2\gamma}\mathcal{R}\right) - \frac{4\gamma\beta_3}{\nu^2}. \tag{68}$$

The second equation in (68) implies that

$$H = \left(Y + \frac{4\gamma\beta_3}{\nu^2}\right)\exp\left(-\frac{\nu}{2\gamma}\mathcal{R}\right)$$

is a first integral of the system. We choose $\mathcal{R}$ as the canonical coordinate and appoint $H$ as the Hamiltonian: $H = H(\mathcal{R}, \mathcal{P})$. Here $\mathcal{P}$ is the momentum canonically conjugate to $\mathcal{R}$ (still to be introduced).

The momentum should be defined so that the canonical equation $\dot{\mathcal{R}} = \partial H/\partial\mathcal{P}$ reproduce the equation (27). The two equations coincide if

$$Z = \frac{1}{2\gamma}\frac{\partial Y}{\partial\mathcal{P}}\exp\left(-\frac{\nu}{2\gamma}\mathcal{R}\right). \tag{69}$$

Eliminating $C$ between two equations in (68) we can express $X$ as

$$X = -\frac{\beta_2}{\nu}Y + x, \tag{70}$$

where

$$x = \frac{2}{\beta_2 + 4\beta_4} - \frac{4\gamma\beta_2\beta_3}{\nu^3} - \sigma\mathcal{R} \tag{71}$$

is independent of $Y$. Assume, for definiteness, $\beta_2\beta_4 < 0$. (The case $\beta_2\beta_4 > 0$ can be dealt with in a similar way.) Substituting (69) and (70) in the identity $X^2 + Y^2 + Z^2 = \mathcal{R}^2$, we obtain

$$\left(Y+\frac{\nu}{4\beta_4}x\right)^2+\eta^{-2}\left(\frac{\partial Y}{\partial \mathcal{P}}\right)^2=r^2, \tag{72}$$

where

$$\eta^2=-\frac{16\gamma^2\beta_2\beta_4}{\nu^2}\exp\left(\frac{\nu}{\gamma}\mathcal{R}\right), \quad r^2=\left(\frac{\nu}{4\beta_4}\right)^2x^2-\frac{\nu^2}{4\beta_2\beta_4}\mathcal{R}^2. \tag{73}$$

Since neither of $x$, $\eta$, or $r$ depends on $Y$, (72) is a separable differential equation for $Y(\mathcal{P})$. A particular solution is $Y=r\sin(\eta\mathcal{P})-\nu(4\beta_4)^{-1}x$. This relation defines $\mathcal{P}$:

$$\mathcal{P}=\frac{1}{\eta}\arcsin\left[\frac{1}{r}\left(Y+\frac{\nu}{4\beta_4}x\right)\right].$$

Lastly, we write the Hamilton function in terms of the canonical variables:

$$H(\mathcal{R},\mathcal{P})=\left[r\sin(\eta\mathcal{P})-\frac{\nu}{4\beta_4}x+\frac{4\gamma\beta_3}{\nu^2}\right]\exp\left(-\frac{\nu}{2\gamma}\mathcal{R}\right),$$

where the coefficients $x(\mathcal{R})$, $\eta(\mathcal{R})$, and $r(\mathcal{R})$ are as in (71) and (73). The two-dimensional manifold $\rho=0$ consists of trajectories of the Hamiltonian system $\dot{\mathcal{R}}=\partial H/\partial\mathcal{P}$, $\dot{\mathcal{P}}=-\partial H/\partial\mathcal{R}$. Individual trajectories are only different in the value of $H$.

## 7. Singular straight-gradient dimer: $\omega^2=0$

Finally we discuss the class of dimers with $\omega^2=0$. (We remind that $\omega^2=\beta_2(\beta_2+4\beta_4)$.) The straight-gradient dimer with $\beta_2=0$ is gauge-equivalent to a cross-gradient system with $u$ and $v$ as canonical variables (section 3). Therefore it remains to consider the case $\beta_2+4\beta_4=0$ with $\beta_2\neq 0$ only.

We start with uncovering the Hamiltonian structure of the singular dimer with an arbitrary coefficient $\beta_3$ (subsection 7.1). In the special case where $\beta_3=0$, the dimer admits an alternative, coexisting, Hamiltonian formulation. This is considered in subsection 7.2.

### *7.1. General singular dimer: arbitrary value of $\beta_3$*

The general solution of equation (28) with $\omega=0$ has the form

$$X=-\frac{\beta_2}{2\gamma}Y_0\mathcal{R}+\frac{\beta_2}{4\gamma^2}\mathcal{R}^2-\frac{\beta_2\beta_3}{12\gamma^2}\mathcal{R}^3+X_0, \tag{74a}$$

$$Y=-\frac{1}{\gamma}\mathcal{R}+\frac{\beta_3}{2\gamma}\mathcal{R}^2+Y_0, \tag{74b}$$

where $X_0$ and $Y_0$ are constants of integration. We define our first canonical variable by

$$y=Y+\frac{1}{\gamma}\mathcal{R}-\frac{\beta_3}{2\gamma}\mathcal{R}^2. \tag{75}$$

According to (74*b*), $y$ is conserved: $y=Y_0$. As in the nonsingular situation, the advantage of using the first integral as a canonical coordinate is that the associated momentum $P_y$ drops out of the dynamics.

Appointing $\mathcal{R}$ as the second canonical coordinate, we need to determine the expression for the momentum $P_{\mathcal{R}}$ canonically conjugate to $\mathcal{R}$. To simplify the notation, we denote it $\mathcal{P}$.

Note that $X$ is not an independent variable here; instead, $X = X(y, \mathcal{R}, \mathcal{P})$. Also note the expression for the $Y$ component of the Stokes vector:

$$Y = y - \frac{1}{\gamma}\mathcal{R} + \frac{\beta_3}{2\gamma}\mathcal{R}^2. \tag{76}$$

We define the Hamiltonian by

$$H = X + \frac{\beta_2}{2\gamma}y\mathcal{R} - \frac{\beta_2}{4\gamma^2}\mathcal{R}^2 + \frac{\beta_2\beta_3}{12\gamma^2}\mathcal{R}^3. \tag{77}$$

The fact that $H$ is a conserved quantity follows from equation (74*a*): $H = X_0$. To identify the momentum $P_{\mathcal{R}} = \mathcal{P}$, we compare the Hamilton equation

$$\dot{\mathcal{R}} = \frac{\partial H}{\partial \mathcal{P}}$$

to equation (27). Since $\partial H/\partial \mathcal{P} = \partial X/\partial \mathcal{P}$, this comparison yields

$$Z = \frac{1}{2\gamma}\frac{\partial X}{\partial \mathcal{P}}. \tag{78}$$

Substituting (76) and (78) in the identity $X^2 + Y^2 + Z^2 = \mathcal{R}^2$, we obtain an ordinary differential equation for $X(\mathcal{P})$:

$$X^2 + \frac{1}{4\gamma^2}\left(\frac{\partial X}{\partial \mathcal{P}}\right)^2 = r^2, \tag{79}$$

where we have introduced

$$r(y, \mathcal{R}) = \sqrt{\mathcal{R}^2 - \left(y - \frac{1}{\gamma}\mathcal{R} + \frac{\beta_3}{2\gamma}\mathcal{R}^2\right)^2}.$$

Note that $r$ is independent of $\mathcal{P}$.

A particular solution of (79) is

$$X = r\,\sin(2\gamma\mathcal{P});$$

then

$$Z = r\,\cos(2\gamma\mathcal{P}).$$

These equations define the momentum $P_{\mathcal{R}}$:

$$P_{\mathcal{R}} = \mathcal{P} = \frac{1}{2\gamma}\,\arctan\left(\frac{X}{Z}\right). \tag{80}$$

On the other hand, the momentum $P_y$ is defined by the canonical equation

$$\dot{P}_y = -\frac{\partial H}{\partial y}.$$

Since $\partial H/\partial P_y = 0$, the right-hand side is independent of $P_y$ and the momentum is recovered by a simple integration: $P_y = -\int(\partial H/\partial y)\mathrm{d}t$.

To complete the identification of the Hamiltonian structure of the singular dimer, we express the Hamilton function in canonical variables:

$$H(y,\,\mathcal{R},\,\mathcal{P})=\frac{\beta_2}{2\gamma}\mathcal{R}\left(y-\frac{1}{2\gamma}\mathcal{R}+\frac{\beta_3}{6\gamma}\mathcal{R}^2\right)+\sin(2\gamma\mathcal{P})\sqrt{\mathcal{R}^2-\left(y-\frac{1}{\gamma}\mathcal{R}+\frac{\beta_3}{2\gamma}\mathcal{R}^2\right)^2}\,.$$

### *7.2. Special singular dimer:* $\beta_3=0$

In this subsection, we consider a special subclass of singular dimers where $\beta_3=0$ is satisfied along with $\beta_2+4\beta_4=0$. Setting $\beta_3=0$ and using (74*b*) to eliminate $Y_0$ from (74*a*), the solution (74) becomes

$$X=-\frac{\beta_2}{4\gamma^2}\mathcal{R}^2-\frac{\beta_2}{2\gamma}Y\mathcal{R}+X_0,\qquad Y=-\frac{1}{\gamma}\mathcal{R}+Y_0. \tag{81}$$

This time, we choose Hamilton's function $H$ to be a multiple of $Y_0$:

$$H=-\gamma Y-\mathcal{R}, \tag{82}$$

and define a canonical coordinate $\rho$ as a quadratic combination of $X$ and $Y$:

$$\rho=\beta_2 Y^2-4X. \tag{83}$$

Using (81), one readily verifies that $\rho$ is a first integral: $\rho=\beta_2 Y_0^2-4X_0$.

Appointing $Y$ as the second canonical coordinate, the associated momentum $P_Y=\mathcal{P}$ should be introduced so as to satisfy the canonical equation $\dot{Y}=\partial H/\partial\mathcal{P}$. The conjugate equation $\dot{\mathcal{P}}=-\partial H/\partial Y$ will then be satisfied automatically. Comparing $\dot{Y}=\partial H/\partial\mathcal{P}$ to (26*b*) and making use of (82) gives

$$\frac{\partial\mathcal{R}}{\partial\mathcal{P}}=2Z. \tag{84}$$

With the help of equation (84), the identity $\mathcal{R}^2-Z^2=X^2+Y^2$ becomes

$$\mathcal{R}^2-\frac{1}{4}\left(\frac{\partial\mathcal{R}}{\partial\mathcal{P}}\right)^2=r^2, \tag{85}$$

where $r$ stands for $\sqrt{X^2+Y^2}$. Using (83), $X$ can be expressed in terms of the independent coordinates $Y$ and $\rho$. This means that $r$ is a function of $Y$ and $\rho$—but does not depend on $\mathcal{P}$:

$$r^2=\frac{1}{16}\left(\beta_2 Y^2-\rho\right)^2+Y^2.$$

Accordingly, equation (85) can be considered as a differential equation for $\mathcal{R}(\mathcal{P})$.

A simple solution to this separable equation is

$$\mathcal{R}=r\cosh(2\mathcal{P}). \tag{86*a*}$$

Equation (84) gives then

$$Z=r\sinh(2\mathcal{P}). \tag{86*b*}$$

The relations (86) define the momentum: $\mathcal{P}=\frac{1}{2}\operatorname{arctanh}(Z/\mathcal{R})$.

Thus the singular dimer with $\beta_3=0$ and $\beta_2+4\beta_4=0$ is a Hamiltonian system with the Hamilton function

$$H=-\gamma Y-\frac{\cosh(2\mathcal{P})}{4}\sqrt{\left(\beta_2 Y^2-\rho\right)^2+16Y^2},$$

canonical coordinates $\rho$ and $Y$, canonical momentum $P_Y=\mathcal{P}$ defined by (86), and the momentum $P_\rho$ recoverable from $\dot{P}_\rho=-\partial H/\partial\rho$. This Hamiltonian formulation coexists with the formulation derived in the previous subsection.

## 8. Nonlinearity-induced $\mathcal{PT}$-symmetry restoration

That some conservative systems have all their trajectories confined to a finite part of the phase space, is a common knowledge. The harmonic oscillator provides a textbook example of this behaviour.

Systems with balanced gain and loss may have a similar property. Assume, for instance, that the amplitudes $u$ and $v$ in (13) and (21) are small. Then these $\mathcal{PT}$-symmetric dimers reduce to a two-site linear Schrödinger equation:

$$\mathrm{i}\dot{u} + v = \mathrm{i}\gamma u, \quad \mathrm{i}\dot{v} + u = -\mathrm{i}\gamma v.$$

When $\gamma$ is small, all solutions to this system are bounded but as $\gamma$ exceeds the critical value of $\gamma_c = 1$, generic initial conditions lead to solutions that grow exponentially (with the growth rate $\lambda = \sqrt{\gamma^2 - 1} > 0$). It is common to say that the $\mathcal{PT}$ symmetry is spontaneously broken in the domain $\gamma \geqslant \gamma_c$ (where solutions blow up) and unbroken in the region $\gamma < \gamma_c$ (where all trajectories are confined). The system is said to undergo the $\mathcal{PT}$-symmetry breaking transition as $\gamma$ is raised through $\gamma_c$ [11–13].

Adding nonlinear terms may bring about a variety of effects. Thus, the on-site nonlinearity of the standard dimer (7) promotes the blow-up. In this system, large enough initial conditions trigger exponential growth regardless of the value of $\gamma$ [33, 34]; furthermore, when $\gamma \geqslant 1$, *all* generic initial conditions blow up [34, 36]. In contrast, the nonlinear coupling of the cross-gradient dimer (6) softens the symmetry-breaking transition. In this case stable bounded solutions persist for arbitrarily large values of the gain–loss coefficient [17]. (A similar effect is exhibited by couples of damped–antidamped anharmonic oscillators [38] and solitons in a defocusing nonlinear trap with symmetrically distributed gain and loss [39]; hence the nonlinear softening is a general phenomenon not limited to dimers.)

In what follows, we show that there are several classes of cross-gradient and straight-gradient $\mathcal{PT}$-symmetric dimers that confine all their trajectories—*regardless of the value of the gain–loss parameter* $\gamma$. In these cases the nonlinearity not just softens the symmetry-breaking transition but suppresses it completely. The $\mathcal{PT}$-symmetry becomes spontaneously restored.

The spontaneous symmetry restoration employs the same mechanism as the transition softening—just in a more efficient way. The exponential growth of small initial conditions is curbed by the nonlinear coupling which diverts increasingly large amounts of energy from the gaining to the losing site. As a result, the blow-up is arrested and all trajectories remain trapped in a finite part of the phase space. (Previously, a similar blow-up suppression was observed in a damped-driven dimer without the $\mathcal{PT}$ symmetry, namely, in the actively coupled waveguide pair [34, 40].)

### 8.1. Cross-gradient dimer

We start with the family of the cross-gradient dimers (13). Each member of the family has two independent constants of motion, $X$ and $\mathfrak{H}$, where the Hamiltonian (12) has the following expression in terms of the Stokes variables:

$$\mathfrak{H} = \alpha_1 \mathcal{R}^2 + \left(\frac{\alpha_2}{4} + \alpha_4\right) X^2 + \alpha_3 X R + \frac{\alpha_2}{4} Y^2 - \mathcal{R} - \gamma Y. \tag{87}$$

Assume, first, that $\alpha_2 \leqslant 0$ while $\alpha_1 + \frac{1}{4}\alpha_2 \neq 0$. Noting that $|Y| \leqslant \mathcal{R}$, we obtain a lower bound for $\mathfrak{H}$:

$$\mathfrak{H} \geqslant \left(\alpha_1 - \frac{|\alpha_2|}{4}\right)\left[\mathcal{R} + \frac{\alpha_3 X - \gamma - 1}{2\left(\alpha_1 + \frac{1}{4}\alpha_2\right)}\right]^2 + \left(\alpha_4 + \frac{\alpha_2}{4}\right)X^2 - \frac{(\alpha_3 X - \gamma - 1)^2}{\alpha_2 + 4\alpha_1}. \tag{88}$$

If $\alpha_1$ is greater than $\frac{1}{4}|\alpha_2|$, then, keeping in mind that $X$ is a first integral, this inequality implies that $\mathcal{R}$ is bounded from above by two constants of motion. That is, there exists an $\mathcal{R}_0$ such that $\mathcal{R}(t) \leqslant \mathcal{R}_0$ for all $t \geqslant 0$—the trajectory is trapped in a finite part of the phase space.

To find the Hamiltonian's lower bound in the situation where $\alpha_2 > 0$, we first write equation (87) in the form

$$\mathfrak{H} = \alpha_1\left(\mathcal{R} + \frac{\alpha_3 X - 1}{2\alpha_1}\right)^2 + \frac{\alpha_2}{4}\left(Y - \frac{2\gamma}{\alpha_2}\right)^2 + \left(\frac{\alpha_2}{4} + \alpha_4\right)X^2 - \frac{(\alpha_3 X - 1)^2}{4\alpha_1} - \frac{\gamma^2}{\alpha_2}.$$

This representation is valid if neither $\alpha_1$ nor $\alpha_2$ is zero. Assuming $\alpha_2 > 0$, this gives a lower bound different from (88):

$$\mathfrak{H} \geqslant \alpha_1\left(\mathcal{R} + \frac{\alpha_3 X - 1}{2\alpha_1}\right)^2 + \alpha_4 X^2 - \frac{(\alpha_3 X - 1)^2}{4\alpha_1} - \frac{\gamma^2}{\alpha_2}.$$

If, in addition, $\alpha_1 > 0$, this inequality implies that there is $\mathcal{R}_0$ such that $\mathcal{R}(t) \leqslant \mathcal{R}_0$ for all $t \geqslant 0$.

If $\alpha_2 < 0$ and $\alpha_1 < 0$, or if $\alpha_2 \geqslant 0$ and $\alpha_1 < -\frac{1}{4}\alpha_2$, we can establish the boundedness of $\mathcal{R}(t)$ by considering the lower bound for the integral $-\mathfrak{H}$ instead of $\mathfrak{H}$.

In summary, trajectories of the cross-gradient dimer are confined if either (a) $\alpha_1$ and $\alpha_2$ are both nonzero and have the same sign; (b) $\alpha_1$ and $\alpha_2$ are both nonzero and of the opposite sign, with $|\alpha_2| < 4|\alpha_1|$; (c) $\alpha_1 \neq 0$ while $\alpha_2 = 0$.

### *8.2. Straight-gradient dimer*

Similar analysis can be carried out for the straight-gradient dimer (21). Let, first, $\omega^2 > 0$ and assume that $\mathcal{R} \to \infty$ as $t$ tends to infinity or approaches some finite value $t_0$. Equation (30*a*) gives

$$X = -\sigma\mathcal{R} + O\left(\mathcal{R}^0\right) \quad \text{as } \mathcal{R} \to \infty.$$

This is only consistent with the inequality $|X| \leqslant \mathcal{R}$ if $|\sigma| \leqslant 1$. Consequently, if $|\sigma| > 1$, all trajectories of the straight-gradient dimer have to be confined: $\mathcal{R}(t) \leqslant \mathcal{R}_0$ with some finite $\mathcal{R}_0$.

This conclusion is illustrated by the left column of figure 1 which shows the surface (31) with $|\sigma| < 1, |\sigma| > 1$, and $|\sigma| = 1$. The surface is only seen to be compact in the middle panel, where $|\sigma| > 1$.

Turning to the $\omega^2 < 0$ subfamily and assuming $\mathcal{R} \to \infty$, equation (33*a*) indicates that the coordinate $X$ will grow exponentially in $\mathcal{R}$ if $C$ is nonzero. This is clearly inconsistent with $|X| \leqslant \mathcal{R}$. The only trajectories in (33*a*) that are consistent with this inequality, are those with $C = 0$; here the growth becomes linear in $\mathcal{R}$ as $\mathcal{R} \to \infty$. However if $|\sigma| > 1$, the slope of the asymptote of $X = X(\mathcal{R})$ will be greater than 1. This is, again, incompatible with $|X| \leqslant \mathcal{R}$. Therefore in the case $|\sigma| > 1$ all trajectories have to be bounded: $\mathcal{R}(t) \leqslant \mathcal{R}_0$.

The surfaces (31) with $\omega^2 < 0$ are plotted in figure 1, right column. As in the left column, here we illustrated $|\sigma| < 1, |\sigma| > 1$, and $|\sigma| = 1$. Only the surface with $|\sigma| > 1$ (middle panel) is compact.

It remains to consider the situation $\omega^2 = 0$ which consists of two cases: (a) $\beta_2 = 0$ and (b) $\beta_2 + 4\beta_4 = 0$. In case (a), equations (28) yield

$$X = X_0, \quad Y = \frac{(\beta_2 + 4\beta_4)X_0 - 2}{2\gamma}\mathcal{R} + \frac{\beta_3}{2\gamma}\mathcal{R}^2.$$

As $\mathcal{R} \to \infty$, the expression for $Y$ is only consistent with $|Y| \leqslant \mathcal{R}$ if $\beta_3 = 0$. Therefore if $\beta_3 \neq 0$, the trajectories have to be confined. This is in agreement with the fact that the straight-gradient dimer with $\beta_2 = 0$ is gauge-equivalent to a cross-gradient dimer with $\alpha_1 = \frac{1}{2}\beta_3$ and $\alpha_2 = 0$, while the cross-gradient dimer with $\alpha_2 = 0$ and $\alpha_1 \neq 0$ has been shown to suppress the blowup (see the previous subsection).

Finally, we let $\beta_2 + 4\beta_4 = 0$. To avoid the duplication of results of the previous paragraph, we also require $\beta_2 \neq 0$. Assuming $\mathcal{R} \to \infty$, the exact solution (74) indicates that the $X$ component would have to grow cubically or quadratically in $\mathcal{R}$ if $\beta_3 \neq 0$ or $\beta_3 = 0$, respectively. However, neither cubic nor quadratic growth is consistent with the inequality $|X| \leqslant \mathcal{R}$. Hence in the case where $\beta_2 + 4\beta_4 = 0$ but $\beta_2 \neq 0$, all trajectories have to be bounded: $\mathcal{R}(t) \leqslant \mathcal{R}_0$.

To illustrate this conclusion geometrically, we depict the solution surface for the case $\beta_2 + 4\beta_4 = 0$. Eliminating $Y_0$ between (74*a*) and (74*b*) gives

$$X - \frac{\beta_2\beta_3}{6\gamma^2}\mathcal{R}^3 + \frac{\beta_2}{4\gamma^2}\mathcal{R}^2 + \frac{\beta_2}{2\gamma}\mathcal{R}Y = X_0. \tag{89}$$

For each $X_0$, equation (89) describes a surface in the $(X, Y, Z)$ space which hosts a one-parameter family of trajectories. If $\beta_3 \neq 0$ and $\beta_2 \neq 0$, the surface is compact (figure 2(a)) so all trajectories are confined to a finite part of the space.

When $\beta_3 = 0$, the surface (89) with a sufficiently large $\gamma$ ($\gamma > \frac{1}{2}$) is noncompact; yet the self-trapping of trajectories can be illustrated in this case as well. To this end, we note that the equation (74*a*) also defines a surface in the $(X, Y, Z)$ space. For the given $X_0$ and $Y_0$, this surface hosts a single trajectory of the dimer. When $\beta_3 = 0$ (while $\beta_2 \neq 0$), the surface (74*a*) is compact—for any $\gamma$ and any choice of $X_0$ and $Y_0$. This is illustrated in figure 2(b).

To summarize, trajectories of the straight-gradient dimer are confined if either (a) $\beta_2(\beta_2 + 4\beta_3) \neq 0$ and $2|\beta_3| > |\beta_2 + 4\beta_4|$; (b) $\beta_2 = 0$ but $\beta_3 \neq 0$; or (c) $\beta_2 + 4\beta_4 = 0$ but $\beta_2 \neq 0$.

## 9. A note on applications

The standard dimer (7) describes the coupling of a Kerr optical waveguide with loss to a twin waveguide characterized by the optical gain of equal rate [2, 3, 10–13]. In the boson condensation context, the same pair of equations governs condensates in two identical potential wells [4], with one well losing and the other one being fed with atoms [14, 15]. The cross-gradient dimer (6) models the same potential-well geometry of the condensate, the difference from the standard dimer being that this time $u$ and $v$ are the amplitudes of the symmetric and antisymmetric state [5] rather than the amplitudes of the condensate in the left and right well.

The aim of this section is to emphasise that other nonlinear models in (13) and (21) are not physically irrelevant either. In particular, these dimers furnish amplitude equations for couples of oscillators with physically realistic nonlinearities. We exemplify this correspondence by simple systems with the gain–loss balance of two different types.

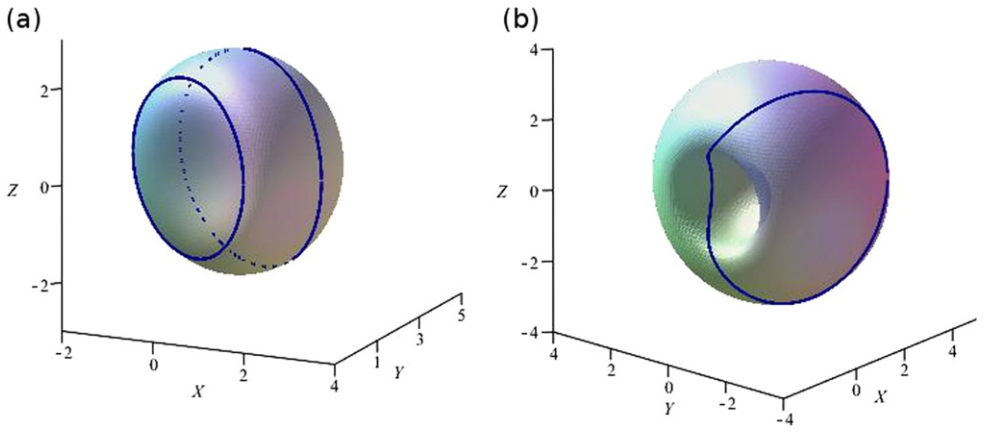


**Figure 2.** (a) The surface (89) with $\beta_2\beta_3 \neq 0$. In this plot, $\gamma = 1$, $\beta_2 = 4$, $\beta_3 = 1$, $\beta_4 = -1$, and $X_0 = 3$. Also shown are two trajectories of the system (26). (b) The surface (74*a*) with $\beta_3 = 0$. Here, $\gamma = 1$, $\beta_2 = 4$, $X_0 = 3$ and $Y_0 = 2$. This surface carries only one trajectory of the system (26) (depicted).

### *9.1. Two pendula with periodic coupling*

The first system consists of two pendula with a periodically varied coupling:

$$\frac{\mathrm{d}^2x}{\mathrm{d}\tau^2} + \sin x + \kappa(\tau)y = 0, \quad \frac{\mathrm{d}^2y}{\mathrm{d}\tau^2} + \sin y + \kappa(\tau)x = 0. \tag{90}$$

The coupling is assumed to be weak and varied at the frequency close to the double natural frequency of each pendulum:

$$\kappa = 2\epsilon^2 \cos(2\omega\tau), \quad \omega = 1 - \Omega\epsilon^2.$$

Here $\epsilon^2$ is a small parameter that sets the scale of the amplitude of the coupling modulation, while the coefficient $\Omega = O(1)$ measures the detuning of the driving half-frequency from the frequency of the linear oscillations.

This type of parametric driving can be easily realized experimentally. For example, the pendula can be hung from a common horizontal rope, with a periodically varied rope tension.

Assuming that the pendula are performing small-amplitude librations, we expand $x$ and $y$ in powers of $\epsilon$:

$$x = \epsilon x_1 + \epsilon^3 x_3 + \ldots, \quad y = \epsilon y_1 + \epsilon^3 y_3 + \ldots .$$

The coefficients of the expansion are allowed to depend on a hierarchy of time scales $T_n = \epsilon^n\omega\tau$, $n = 0, 2, \ldots$. The times $T_n$ become independent as $\epsilon \to 0$; in this limit, $\mathrm{d}/\mathrm{d}\tau = \omega(D_0 + \epsilon^2 D_2 + \ldots)$, where $D_n = \partial/\partial T_n$. We also develop $\sin x$ and $\sin y$ in powers of their arguments.

Substituting these expansions in (90) and equating coefficients of like powers of $\epsilon$, the order $\epsilon^1$ yields

$$x_1 = A\mathrm{e}^{\mathrm{i}T_0} + A^*\mathrm{e}^{-\mathrm{i}T_0}, \quad y_1 = \mathrm{i}B\mathrm{e}^{\mathrm{i}T_0} - \mathrm{i}B^*\mathrm{e}^{-\mathrm{i}T_0},$$

where $A$ and $B$ are functions of $T_2$, $T_4$ ,...—but not of $T_0$. At the order $\epsilon^3$ we obtain a pair of equations

$$\left(D_0^2+1\right)x_3 = 2\Omega D_0^2 x_1 - 2D_0D_2x_1 - 2\cos\left(2T_0\right)y_1 + \frac{1}{6}x_1^3,$$
$$\left(D_0^2+1\right)y_3 = 2\Omega D_0^2 y_1 - 2D_0D_2y_1 - 2\cos\left(2T_0\right)x_1 + \frac{1}{6}y_1^3.$$

Substituting for $x_1$ and $y_1$, and setting the secular term equal to zero we arrive at

$$2\mathrm{i}D_2A + 2\Omega A - \mathrm{i}B^* - \frac{1}{2}|A|^2A = 0,$$
$$2\mathrm{i}D_2B + 2\Omega B - \mathrm{i}A^* - \frac{1}{2}|B|^2B = 0. \tag{91}$$

Assuming, for definiteness, $\Omega > 0$ and letting

$$A = 2\sqrt{\Omega}\,(u+v), \quad B = 2\sqrt{\Omega}\left(u^*-v^*\right),$$

equation (91) become

$$\mathrm{i}\dot{u} + v - \mathrm{i}\gamma u = u^2v^* + \left(2|u|^2+|v|^2\right)v,$$
$$\mathrm{i}\dot{v} + u + \mathrm{i}\gamma v = v^2u^* + \left(2|v|^2+|u|^2\right)u, \tag{92}$$

where we have introduced $\gamma = (2\Omega)^{-1}$ and the overdot indicates differentiation with respect to $t = \Omega T_2$. The system (92) is nothing but the cross-gradient $\mathcal{PT}$-symmetric dimer (13) with $\alpha_2 = \alpha_3 = 0$ and $\alpha_1 = \alpha_4 = \frac{1}{2}$.

### *9.2. Damped–antidamped oscillator couples*

Another, unrelated, interpretation of equations (13) and (21) is that of amplitude equations for a damped oscillator coupled to an oscillator with negative damping. (This time the coupling coefficient is assumed to be constant.) Following the multiple-scale procedure of the previous subsection, one can readily check that the cross-gradient dimer (13) governs the oscillation amplitudes of the damped–antidamped pair

$$x_{\tau\tau} + \eta x_\tau + x + \kappa y = c_0\left(x^2+3y^2\right)x + \left(c_1x^2+c_2y^2\right)y,$$
$$y_{\tau\tau} - \eta y_\tau + y + \kappa x = c_0\left(y^2+3x^2\right)y + \left(c_1y^2+c_2x^2\right)x. \tag{93}$$

Here $\kappa = \epsilon^2$ and $\eta = \gamma\epsilon^2$ are the coupling and the gain–loss coefficient (assumed small), while the nonlinearity coefficients $c_0$, $c_1$ and $c_2$ can be chosen arbitrarily. The dimer parameters in (13) are expressible through the coefficients in (93): $\alpha_1 = \frac{3}{2}c_2$, $\alpha_2 = c_1 - 3c_2$, $\alpha_3 = 3c_0$, and $\alpha_4 = \frac{1}{2}c_1$.

On the other hand, the straight-gradient dimer (21) serves as the amplitude system for the oscillator couple

$$x_{\tau\tau} + \eta x_\tau + x + \kappa y = \left(c_1x^2+c_2y^2\right)x + c_0\left(3x^2+y^2\right)y,$$
$$y_{\tau\tau} - \eta y_\tau + y + \kappa x = \left(c_1y^2+c_2x^2\right)y + c_0\left(3y^2+x^2\right)x.$$

This time, the relation between the coefficients of the oscillators and the dimer parameters is as follows: $\beta_1 = \frac{3}{2}c_1$, $\beta_2 = c_2 - 3c_1$, $\beta_3 = 3c_0$, and $\beta_4 = \frac{1}{2}c_2$.

The damped–antidamped oscillator model has been employed to interpret experiments in systems as diverse as a tied pair of magnetically kicked pendula [41], two connected optical whispering galleries [16, 42], or a tandem of inductively coupled active *LRC* circuits—one with amplification and the other one attenuated at an equal rate [43].

## 10. Conclusions

The main results of this study can be summarized as follows.

(1) We have introduced a four-parameter ($\alpha_1$, $\alpha_2$, $\alpha_3$, $\alpha_4$) family of Hamiltonian $\mathcal{PT}$-symmetric dimers with a cross-gradient canonical structure, equation (13). The entire family was shown to have an additional integral of motion, independent of the Hamiltonian; hence each member of the family is Liouville integrable. All trajectories in these systems were described analytically.

(2) We have considered a $\mathcal{PT}$-symmetric extension of a four-parameter ($\beta_1$, $\beta_2$, $\beta_3$, $\beta_4$) family of conservative dimers with the straight-gradient Hamiltonian structure, equation (21). Unlike for the cross-gradient dimers, the original complex $u$, $v$ variables do not constitute canonical coordinates for the straight-gradient family (21)—except when the straight-gradient dimer has a coexisting cross-gradient formulation. The three-parameter ($\beta_1$, $\beta_3$, $\beta_4$) subfamily of straight-gradient dimers with $\beta_2 = 0$ was shown to admit such an alternative cross-gradient representation.
We have identified canonical coordinates and momenta and uncovered the Hamiltonian structure for the entire four-parameter family of the straight-gradient $\mathcal{PT}$-symmetric dimers. By establishing that each member of the family has an additional integral of motion, we have demonstrated that the entire family is Liouville integrable. All trajectories of the straight-gradient $\mathcal{PT}$-symmetric dimers were described analytically.

(3) We have proved that the cross-gradient dimer with parameters $\alpha_{1,2}$ satisfying (a) $\alpha_1\alpha_2 > 0$; or (b) $\alpha_1\alpha_2 < 0$ with $|\alpha_2| < 4\,|\alpha_1|$; or (c) $\alpha_1 \neq 0$ while $\alpha_2 = 0$—has all trajectories bounded, irrespectively of the values of other parameters $\alpha_{3,4}$ or the gain–loss coefficient $\gamma$.

(4) We have established that regardless of the value of $\beta_1$ and the gain–loss coefficient $\gamma$, the straight-gradient dimer with parameters satisfying (a) $\beta_2(\beta_2 + 4\beta_3) \neq 0$, $2\,|\beta_3| > |\beta_2 + 4\beta_4|$; or (b) $\beta_2 = 0$, $\beta_3 \neq 0$, with no constraints on $\beta_4$; or (c) $\beta_2 + 4\beta_4 = 0$, $\beta_2 \neq 0$, with no constraints on $\beta_3$—has all trajectories bounded.

(5) We have demonstrated that the amplitudes of libration of two coupled oscillators with on-site nonlinearities, driven by the periodic variation of their coupling coefficient, satisfy a $\mathcal{PT}$-symmetric cross-gradient dimer system. □

Thus, the principal mathematical conclusion is that the $\mathcal{PT}$-symmetric extensions of *all* conservative nonlinear Schrödinger dimers remain completely integrable Hamiltonian systems. On the other hand, the principal physical upshot is that there are broad classes of $\mathcal{PT}$-symmetric dimers that confine all their trajectories *regardless of the value of the gain–loss parameter* $\gamma$. The $\mathcal{PT}$-symmetry, which is broken at the level of the underlying linear equation, becomes spontaneously restored thanks to the nonlinear coupling.

The spontaneous $\mathcal{PT}$-symmetry restoration may find applications in integrated optics where $\mathcal{PT}$-symmetric nonlinear Schrödinger dimers describe directional waveguide couplers. A nonlinear coupler composed of one core with a certain amount of optical gain and another one with an equal amount of loss switches the entire power to one waveguide [3]. In the standard $\mathcal{PT}$ dimer, this power switching is accompanied by an unbounded power growth in one of the arms of the device—the growth not saturable by nonlinearity [12, 13, 23, 37]. In contrast, no input can trigger an uncontrollable growth of optical modes in a dimer with the nonlinearly-restored $\mathcal{PT}$ symmetry. As a result, the $\mathcal{PT}$ symmetry restoration may represent a technological advantage.

## Acknowledgments

This project began during one of the authors (D E P's) visit to the University of Cape Town in April 2014. He would like to thank the Visiting Scholars Fund of UCT for financial support. The work of P D was funded through a postdoctoral fellowship from the Claude Leon Foundation. I B acknowledges research funding from the NRF of South Africa (grants No 85751, 86991, and 87814). The work of D E P was supported by the Ministry of Education and Science of Russian Federation (the base part of the state task No. 2014/133, project No. 2839). Last but not least, it is a pleasure to thank Vladimir Konotop, Tsampikos Kottos, Boris Malomed, Philip Mannheim and Vyacheslav Priezzhev for useful discussions.

## References

[1] Jensen S 1982 The nonlinear coherent coupler *IEEE J. Quantum Electron.* **18** 1580–3
Maier A A 1982 Optical transistors and bistable devices utilizing nonlinear transmission of light in systems with undirectional coupled waves *Sov. J. Quantum Electron.* **12** 1490–4
[2] Maier A A 1987 Possible practical use of self-switching of radiation in coupled waveguides for amplification of the useful modulation of a signal *Sov. J. Quantum Electron.* **17** 1013–8
Maier A A 1995 Optical self-switching of unidirectional distributively coupled waves *Phys.-Usp* **38** 991–1031
[3] Chen Y, Snyder A W and Payne D N 1992 Twin core nonlinear couplers with gain and loss *IEEE J. Quantum Electron.* **28** 239–45
[4] Milburn G J, Corney J, Wright E M and Walls D F 1997 Quantum dynamics of an atomic Bose–Einstein condensate in a double-well potential *Phys. Rev.* A **55** 4318–25
Smerzi A, Fantoni S, Giovanazzi S and Shenoy S R 1997 Quantum coherent atomic tunneling between two trapped Bose–Einstein condensates *Phys. Rev. Lett.* **79** 4950–4
Raghavan S, Smerzi A, Fantoni S and Shenoy S R 1999 Coherent oscillations between two weakly coupled Bose–Einstein condensates: Josephson effects, $\pi$ oscillations, and macroscopic quantum self-trapping *Phys. Rev.* A **59** 620–34
[5] Ostrovskaya E A, Kivshar Y S, Lisak M, Hall B, Cattani F and Anderson D 2000 Coupled-mode theory for Bose–Einstein condensates *Phys. Rev.* A **61** 031601
Ananikian D and Bergeman T 2006 Gross–Pitaevskii equation for Bose particles in a double-well potential: two-mode models and beyond *Phys. Rev.* A **73** 013604
Theocharis G, Kevrekidis P G, Frantzeskakis D J and Schmelcher P 2006 Symmetry breaking in symmetric and asymmetric double-well potentials *Phys. Rev.* E **74** 056608
[6] Eilbeck J C, Lomdahl P S and Scott A C 1985 The discrete self-trapping equation *Physica* D **16** 318–38
[7] Kenkre V M and Campbell D K 1986 Self-trapping on a dimer: time-dependent solutions of a discrete nonlinear Schrödinger equation *Phys. Rev.* B **34** 4959–62
Scott A C, Eilbeck J C and Gilhoj H 1994 Quantum lattice solitons *Physica* D **78** 194–213
[8] Hennig D and Tsironis G P 1999 Wave transmission in nonlinear lattices *Phys. Rep.* **307** 333–432
[9] Bender C M and Boettcher S 1998 Real spectra in Non-Hermitian Hamiltonians having $\mathcal{PT}$-symmetry *Phys. Rev. Lett.* **80** 5243–7
Bender C M 2005 Introduction to $\mathcal{PT}$-symmetric quantum theory *Contemp. Phys.* **46** 277–92
Bender C M 2007 Making sense of non-Hermitian Hamiltonians *Rep. Prog. Phys.* **70** 947–1018
Mostafazadeh A 2010 Pseudo-Hermitian representation of quantum mechanics *Int. J. Geom. Methods Mod. Phys.* **7** 1191–307
[10] Kulishov M, Laniel J M, Bélanger N, Azaña M and Plant D V 2005 Nonreciprocal waveguide Bragg gratings *Opt. Express* **13** 3068–78
El-Ganainy R, Makris K G, Christodoulides D N and Musslimani Z H 2007 Theory of coupled optical $\mathcal{PT}$-symmetric structures *Opt. Lett.* **32** 2632–4
[11] Guo A, Salamo G J, Duchesne D, Morandotti R, Volatier-Ravat M, Aimez V, Siviloglou G A and Christodoulides D N 2009 Observation of $\mathcal{PT}$-symmetry breaking in complex optical potentials *Phys. Rev. Lett.* **103** 093902

[12] Rüter C E, Makris K G, El-Ganainy R, Christodoulides D N, Segev M and Kip D 2010 Observation of parity-time symmetry in optics *Nat. Phys.* **6** 192–5
Kottos T 2010 Optical physics: broken symmetry makes light work *Nat. Phys.* **6** 166–7
[13] Ramezani H, Kottos T, El-Ganainy R and Christodoulides D N 2010 Unidirectional nonlinear $\mathcal{PT}$-symmetric optical structures *Phys. Rev.* A **82** 043803
[14] Graefe E M, Korsch H J and Niederle A E 2008 Mean-field dynamics of a non-Hermitian Bose-Hubbard dimer *Phys. Rev. Lett.* **101** 150408
Graefe E M, Korsch H J and Niederle A E 2010 Quantum-classical correspondence for a non-Hermitian Bose-Hubbard dimer *Phys. Rev.* A **82** 013629
Graefe E M 2012 Stationary states of a $\mathcal{PT}$-symmetric two-mode Bose–Einstein condensate *J. Phys. A: Math. Theor.* **45** 444015
[15] Heiss W D, Cartarius H, Wunner G and Main J 2013 Spectral singularities in $\mathcal{PT}$-symmetric Bose–Einstein condensates *J. Phys. A: Math. Theor.* **46** 275307
[16] Bender C M, Gianfreda M, Özdemir Ş K, Peng B and Yang L 2013 Twofold transition in $\mathcal{PT}$-symmetric coupled oscillators *Phys. Rev.* A **88** 062111
[17] Barashenkov I V and Gianfreda M 2014 An exactly solvable $\mathcal{PT}$-symmetric dimer from a Hamltonian system of nonlinear oscillators with gain and loss *J. Phys. A: Math. Theor.* **47** 282001
[18] Barashenkov I V 2014 Hamiltonian formulation of the standard $\mathcal{PT}$-symmetric nonlinear Schrödinger dimer *Phys. Rev.* A **90** 045802
[19] Martínez A J, Molina M I, Turitsyn S K and Kivshar Y S 2015 Nonlinear multi-core waveguiding structures with balanced gain and loss *Phys. Rev.* A **91** 023822
[20] Jørgensen M F, Christiansen P L and Abou-Hayt I 1993 On a modified discrete self-trapping dimer *Physica* D **68** 180–4
Jørgensen M F and Christiansen P L 1994 Hamiltonian structure for a modified discrete self-trapping dimer *Chaos Solitons Fractals* **4** 217–25
Jørgensen M F and Christiansen P L 1998 Self-trapping and blow-up in integrable dimers *J. Phys. A: Math. Gen.* **31** 969–77
[21] Klaiman S, Günther U and Moiseyev N 2008 Visualization of branch points in $\mathcal{PT}$-symmetric waveguides *Phys. Rev. Lett.* **101** 080402
[22] Peng B, Özdemir Ş, Lei F, Monifi F, Gianfreda M, Long G, Fan S, Nori F, Bender C M and Yang L 2014 Parity-time-symmetric whispering-gallery microcavities *Nat. Phys.* **10** 394–8
[23] Lin Z, Ramezani H, Eichelkraut T, Kottos T, Cao H and Christodoulides D N 2011 Unidirectional invisibility induced by $\mathcal{PT}$-symmetric periodic structures *Phys. Rev. Lett.* **106** 213901
Regensburger A, Bersch C, Miri M A, Onishchukov G, Christodoulides D N and Peschel U 2012 Parity-time synthetic photonic lattices *Nature* **488** 167–71
[24] Chugunova M and Pelinovsky D E 2006 Block-diagonalization of the symmetric first-order coupled-mode system *SIAM J. Appl. Dyn. Syst.* **5** 66–83
[25] Aceves A B and Wabnitz S 1989 Self-induced transparency solitons in nonlinear refractive periodic media *Phys. Lett.* A **141** 37–42
Barashenkov I V, Pelinovsky D E and Zemlyanaya E V 1998 Vibrations and oscillatory instabilities of gap solitons *Phys. Rev. Lett.* **80** 5117–21
[26] Kuznetsov E A and Mikhailov A V 1977 On the complete integrability of the two-dimensional classical-Thirring model *Theor. Math. Phys.* **30** 193–200
Barashenkov I V and Getmanov B S 1993 The unified approach to integrable relativistic equations: soliton solutions over nonvanishing backgrounds II *J. Math. Phys.* **34** 3054–73
[27] Blanchard P, Stubbe J and Vàzquez L 1987 Stability of nonlinear spinor fields with application to the Gross–Neveu model *Phys. Rev.* D **36** 2422–9
[28] David D 1984 On an extension of the classical-Thirring model *J. Math. Phys.* **25** 3424–33
[29] Bogolubsky I L 1979 On spinor soliton stability *Phys. Lett.* A **73** 87–90
Alvarez A and Carreras B 1981 Interaction dynamics for the solitary waves of a nonlinear Dirac model *Phys. Lett.* A **86** 327–32
Campbell D K and Bishop A R 1982 Soliton excitations in polyacetylene and relativistic field theory models *Nucl. Phys.* B **200** 297–328
Alvarez A and Soler M 1983 Energetic stability criterion for a nonlinear spinorial model *Phys. Rev. Lett.* **50** 1230–4
[30] Lee S Y, Kuo T K and Gavrielidis A 1975 Exact localized solutions of two-dimensional field theories of massive fermions with Fermi interactions *Phys. Rev.* D **12** 2249–54

[31] Li K and Kevrekidis P G 2011 $\mathcal{PT}$-symmetric oligomers: analytical solutions, linear stability, and nonlinear dynamics *Phys. Rev.* E **83** 066608
Rondrigues A S, Li K, Achilleos V, Kevrekidis P G, Frantzeskakis D J and Bender C M 2013 $\mathcal{PT}$-symmetric double-well potentials revisited: bifurcations, stability and dynamics *Rom. Rep. Phys.* **65** 5–26
Duanmu M, Li K, Horne R L, Kevrekidis P G and Whitaker N 2013 Linear and nonlinear parity-time-symmetric oligomers: a dynamical systems analysis *Phil. Trans. R. Soc.* A **371** 20120171
[32] Cuevas J, Kevrekidis P G, Saxena A and Khare A 2013 $\mathcal{PT}$-symmetric dimer of coupled nonlinear oscillators *Phys. Rev.* A **88** 032108
[33] Kevrekidis P G, Pelinovsky D E and Tyugin D Y 2013 Nonlinear dynamics in $\mathcal{PT}$-symmetric lattices *J. Phys. A: Math. Theor.* **46** 365201
[34] Barashenkov I V, Jackson G S and Flach S 2013 Blow-up regimes in the $\mathcal{PT}$-symmetric coupler and the actively coupled dimer *Phys. Rev.* A **88** 053817
[35] Pelinovsky D E, Zezyulin D A and Konotop V V 2014 Nonlinear modes in a generalized $\mathcal{PT}$-symmetric discrete nonlinear Schrodinger equation *J. Phys. A: Math. Theor.* **47** 085204
[36] Pickton J and Susanto H 2013 On the integrability of $\mathcal{PT}$-symmetric dimers *Phys. Rev.* A **88** 063840
[37] Sukhorukov A A, Xu Z Y and Kivshar Y S 2010 Nonlinear suppression of time reversals in $\mathcal{PT}$-symmetric optical couplers *Phys. Rev.* A **82** 043818
[38] Cuevas-Maraver J, Khare A, Kevrekidis P G, Xu H and Saxena A $\mathcal{PT}$-symmetric dimer in a generalized model of coupled nonlinear oscillators *Int. J. Theor. Phys.* **53**
[39] Kartashov Y V, Malomed B A and Torner L 2014 Unbreakable $\mathcal{PT}$-symmetry of solitons supported by inhomogeneous defocusing nonlinearity *Opt. Lett.* **39** 5641–4
[40] Alexeeva N V, Barashenkov I V, Rayanov K and Flach S 2014 Actively coupled optical waveguides *Phys. Rev.* A **89** 013848
[41] Bender C M, Berntson B K, Parker D and Samuel E 2013 Observation of $\mathcal{PT}$ phase transition in a simple mechanical system *Am. J. Phys.* **81** 173–9
[42] Peng B, Özdemir Ş K, Lei F, Monifi F, Gianfreda M, Long G L, Fan S, Nori F, Bender C M and Yang L 2014 Parity-time-symmetric whispering-gallery microcavities *Nat. Phys.* **10** 394–8
[43] Schindler J, Li A, Zheng M C, Ellis F M and Kottos T 2011 Experimental study of active LRC circuits with $\mathcal{PT}$ symmetries *Phys. Rev.* A **84** 040101(R)